NASA/TM–2013-217993

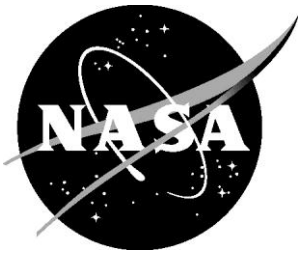

Evaluation of Acoustic Emission SHM of PRSEUS Composite Pressure Cube Tests

Michael R. Horne
National Institute of Aerospace, Hampton, Virginia

Eric I. Madaras
Langley Research Center, Hampton, Virginia

May 2013

NASA STI Program . . . in Profile

Since its founding, NASA has been dedicated to the advancement of aeronautics and space science. The NASA scientific and technical information (STI) program plays a key part in helping NASA maintain this important role.

The NASA STI program operates under the auspices of the Agency Chief Information Officer. It collects, organizes, provides for archiving, and disseminates NASA's STI. The NASA STI program provides access to the NASA Aeronautics and Space Database and its public interface, the NASA Technical Report Server, thus providing one of the largest collections of aeronautical and space science STI in the world. Results are published in both non-NASA channels and by NASA in the NASA STI Report Series, which includes the following report types:

- TECHNICAL PUBLICATION. Reports of completed research or a major significant phase of research that present the results of NASA Programs and include extensive data or theoretical analysis. Includes compilations of significant scientific and technical data and information deemed to be of continuing reference value. NASA counterpart of peer-reviewed formal professional papers, but having less stringent limitations on manuscript length and extent of graphic presentations.

- TECHNICAL MEMORANDUM. Scientific and technical findings that are preliminary or of specialized interest, e.g., quick release reports, working papers, and bibliographies that contain minimal annotation. Does not contain extensive analysis.

- CONTRACTOR REPORT. Scientific and technical findings by NASA-sponsored contractors and grantees.

- CONFERENCE PUBLICATION. Collected papers from scientific and technical conferences, symposia, seminars, or other meetings sponsored or co-sponsored by NASA.

- SPECIAL PUBLICATION. Scientific, technical, or historical information from NASA programs, projects, and missions, often concerned with subjects having substantial public interest.

- TECHNICAL TRANSLATION. English-language translations of foreign scientific and technical material pertinent to NASA's mission.

Specialized services also include organizing and publishing research results, distributing specialized research announcements and feeds, providing information desk and personal search support, and enabling data exchange services.

For more information about the NASA STI program, see the following:

- Access the NASA STI program home page at *http://www.sti.nasa.gov*

- E-mail your question to help@sti.nasa.gov

- Fax your question to the NASA STI Information Desk at 443-757-5803

- Phone the NASA STI Information Desk at 443-757-5802

- Write to:
  STI Information Desk
  NASA Center for AeroSpace Information
  7115 Standard Drive
  Hanover, MD 21076-1320

NASA/TM–2013-217993

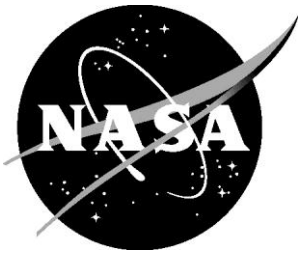

Evaluation of Acoustic Emission SHM of PRSEUS Composite Pressure Cube Tests

Michael R. Horne
National Institute of Aerospace, Hampton, Virginia

Eric I. Madaras
Langley Research Center, Hampton, Virginia

National Aeronautics and
Space Administration

Langley Research Center
Hampton, Virginia 23681-2199

May 2013

Available from:

NASA Center for AeroSpace Information
7115 Standard Drive
Hanover, MD 21076-1320
443-757-5802

Table of Contents

Table of Figures

Symbols and Abbreviations

AE	Acoustic Emission
BWB	Blended Wing Body
COLTS	Combined Loads Test facility
FR	Felicity ratio
LaRC	NASA Langley Research Center
NDE	Nondestructive Evaluation
P	Operating pressure (9.2 psi)
PLB	pencil lead break
PRSEUS	Pultruded Rod Stitched Efficient Unitized Structure
SE	Signal Energy
V	Voltage
V_i	Signal voltage
VIC	Visual Image Correlation

Abstract

A series of tests of the Pultruded Rod Stitched Efficient Unitized Structure (PRSEUS) pressure cube were conducted during third quarter 2011 at NASA Langley Research Center (LaRC) in the Combined Loads Test facility (COLTS). This is a report of the analysis of the Acoustic Emission (AE) data collected during those tests. The AE signals of the later tests are consistent with the final failure progression through two of the pressure cube panels. Calibration tests and "damage precursor" AE indications, from preliminary checkout pressurizations, indicated areas of concern that eventually failed. Hence those tests have potential for vehicle health monitoring.

1.0 Introduction

A cube constructed of Pultruded Rod Stitched Efficient Unitized Structure (PRSEUS) composite panels was pressurized pneumatically at NASA Langley Research Center (LaRC) in the Combined Loads Test facility (COLTS) to increasing levels during a series of tests. The series started with checkout tests to verify the proper operation of all instrumentation and finished with the final test in which internal pressure was increased until final failure. This document describes the investigation of the Acoustic Emission (AE) data collected during these tests.

The PRSEUS concept [1] for the composite structure improves on the state of the art as noted in figure 1 by eliminating fasteners and providing damage arrest while incorporating integral stiffeners for efficient strength to weight ratios. A pultruded rod in a stringer cap perpendicular to foam-core frames is a novel way to create a dry carbon fiber stitched preform that supports itself during vacuum bagging and resin infusion. Fabrication does not require complex interior mold tools [2] so that point-of-fabrication customization for structural changes is easy and inexpensive. The dry multi-ply stacks and sub-structures are stitched together using Vectran fibers into the near final shape for incorporation into the Blended Wing Body (BWB) design.

Figure 2 illustrates a 3-D schematic of a subsection of the large scale BWB test article being realized as the PRSEUS pressure cube test article with a bulkhead panel removed [3]. The cube consists of six sides of PRESUS construction. There are two ribs, two bulkheads, a crown and a floor. Each bulkhead panel is joined to the adjacent sides by bolting it to T-cross-section integral caps. These caps on the surrounding rib, crown, and floor panels capture the panel like a picture frame. Every panel has seven or eight rod stiffened PRSEUS stringers (rib or bulkhead panel, respectively) spaced 6.0 inches apart. These stringers cross perpendicular to two frames spaced 24 inches apart. The spaces of unstiffened panel are called bays. At the corner of two contiguous panels the stringers on one panel do not intersect the stringers of the other. The outside dimensions of the pressure cube are approximately 52 in. x 48 in. x 56 in. [4]

The AE sensors applied to the crown and one of the rib panels, as well as the section of the frame that buckled first during failure, are shown in figure 2. For purposes of illustration the bulkhead panel indicated as "blkhd panel removed for clarity" can be considered as the panel that blew out during failure, leaving the cube looking much as the figure illustrates, albeit, a little more ragged and fractured.

That bulkhead panel (containing AE sensors 1-6) and the indicated rib panel (containing AE sensors 19-26) were painted with black/white speckle pattern. The patterning is for the Visual Image Correlation (VIC) non-contacting full-field strain measurement technique developed by researchers at the University of South Carolina [5, 6]. These panels are described in this document as "VIC" or "speckled" panels. This strain measurement is realized by tracking the deformation of the speckling with two location-calibrated and synchronized cameras for each

panel. The other panels on the cube were painted grey and are described as such in the following discussions.

2.0 Acoustic Emission Collection Test Configuration

Thirty-two acoustic emission sensors (Digital Wave B225.5) were mounted on the outside of the pressure cube as shown in figures 2 and 3. For easy removal all sensors were bonded with Lord 202 acrylic adhesive onto aluminum metal tape that was attached to the test article as seen in figure 4. The diameter of the sensor is approximately 0.75 inches.

Figure 3 shows the numbering scheme for the sensors. This figure is a multiview orthographic projection of all the panels excluding the floor. Each view is a scaled drawing of the stitching pattern for the panel. Each panel contains six sensors, except for the speckled rib panel that has two extra sensors around an applied impact. A 1-inch spherical impactor applied the dropped weight impact of 100 ft-lbs during the test series prior to the final failure pressurization [3]. This illustration allows one to note the location of the AE sensors, which were attached to the smooth outside of the cube, relative to the structural components (stringers, frames, and integral caps) inside the cube. This type of description of the sensor locations is relevant because the significant changes in geometry of the cube at the stiffening elements are more likely to be where damage occurs first. These stiffeners can also act as waveguides to propagate the AE.

All sensors were connected to thin coaxial sensor cables, which in turn were connected to Digital Wave PA0 preamp/line drivers to buffer the weak signal back to the data acquisition system. The preamps were connected via thicker low noise coaxial cables to two Digital Wave FM1 signal conditioning 16-channel amplifiers, which were remotely located in the COLTS control room. The amplifiers were connected to a computer containing multi-channel Digital Wave data acquisition hardware and software. The computer and amplifiers were actively manned during the tests. The data was recorded for subsequent processing with the same software.

A summary of the amplifier gains for the tests is shown in figure 5. Settings did not change until the increase in AE rate and signal strength necessitated a reduction in signal gain to reduce signal amplitude saturation, and/or a reduction in trigger gain to reduce rate saturation and subsequent data loss. A change in signal gain can be compensated for, in post processing under certain conditions, by scaling the amplitude as though acquired at a different gain. However, comparisons between signals cannot be accurate if one signal is amplitude saturated when acquired (i.e. amplitude clipped by a hardware limitation) and the other is not. Calculations such as energy or frequency content acquire errors when the signal is clipped. A reduction in trigger gain is a change that cannot be compensated for, because it involves loss of potentially relevant data that is now below the threshold for triggering data acquisition, but was above the threshold at the higher previous gain. When these changes have occurred, comparing parameters such as total or cumulative AE/energy or AE event rates is not wise. As noted in figure 5, a trigger gain change was implemented when executing AE system check tests (pencil lead break tests) and prior to the “2P” and “Failure” pressurization tests.

3.0 AE Metrics

AE systems collect structure-borne sound, typically not audible, in the ultrasonic frequency band

from 50 to 500 kHz, generated by dynamic processes such as damage initiation and growth in a structure. The technique can be sensitive to rapidly occurring displacements at scales as small as picometers [7]. That sensitivity can monitor pre-cursors to failure in real-time but comes at the cost of differentiating types of real damage from other sources of AE.

For a typical test, data from an array of acoustic sensors located around the structure is acquired. The AE data can be used to locate the epicenter or source location of the damage by triangulation. This requires using the time-of-flight of the sound from the source to the different sensors along with knowledge of the sound wave velocity and sound path. Also typically recorded are the event time and various types of test parameters such as load or pressure. Therefore, one can plot the event rate (events per unit time) as well as the events as a function of those parameters such as load or pressure.

Knowing the velocity of the AE wave propagation accurately is a major factor affecting the accuracy of event location calculations. The simplest unbounded materials are homogeneous and isotropic and have three modes of wave travel with differing velocities. Boundaries support many other modes of wave propagation (plate, surface, etc.). Wave propagation can also be dispersive, particularly in guided waves, where the velocity is a function of frequency. Anisotropy introduces velocity that varies with direction even for the same mode of propagation. Hence, wave velocity can be a function of where the wave is traveling in a material, what direction it is traveling, and its mode of travel. Complex, bounded, inhomogeneous, and anisotropic structures made from various materials can potentially create and sustain many different modes, frequencies and, hence, velocities of propagation. Damage introduces changes in material and mechanical properties that can further affect propagation velocity.

Knowing the arrival times at the sensors accurately is another major factor affecting the accuracy of event location calculations. A low signal to noise ratio makes it more difficult to determine the signal arrival time accurately due to the interference of the noise with the signal. Determining the wave arrival times can also be complicated when there are numerous overlapping arrivals of different wave modes and reflections from different boundaries. Hence, the accuracy of event source location is a function of many variables.

Yet another factor in source location accuracy is the sensor density, or the number of sensors near a given AE event. Typically, the more sensors that detect the event and record the arrival time, the better the estimate obtained for the source location. However, this comes at the cost of requiring additional sensors and instrumentation. For complex structures, one way to limit sensor count is to use a regional or zonal location method where each sensor is positioned in a central location of a region of critical or structural significance. For this sparse distribution of sensors, AE signals from a given source event are typically only detected by a few of the sensors located closest to the event. The location estimate is then a region or zone surrounding the first hit sensor and bounded by either the zones for surrounding sensors or an estimate of the maximum distance a signal might propagate and still be detectable. While this does not provide a pinpoint estimate of damage location, it provides a region in which other NDE techniques are used to more accurately locate and assess the damage.

Another metric is the signal energy contained in the detected acoustic signal acquired at each sensor. This energy of an event is evaluated by calculating the signal energy, *SE*, from the signal as

$$SE = \sum_{i=1}^{n} V_i^2 \Delta t ,$$

where V_i is the signal voltage, i is the time reference point, n is the number of time points in the signal, Δt is the sampling time per point. In other words, the signal energy is the area under the voltage^2-time curve, with units such as $V^2\mu sec$. However, energy in a physical sense is defined as Joules with dimensions of Watt·sec or V^2sec/ohm. To relate signal energy to physical energy E requires including the impedance in ohms of the load driven by the signal. The calculated AE signal energy is related to the energy released in the source event by effects from the transfer function of the material (attenuation, filtering, reflection, etc.) during propagation from source to sensor as well as from the transfer function of the sensor. So the trends in changes of the energy over time, load, or some other experimental variable is more valuable than efforts to get absolute calibrated values for each event.

Material behavior that is related to change of AE over time and load, such as the Kaiser Effect and the Felicity effect, can be used to evaluate damage development. To paraphrase the Nondestructive Testing volume of the ASM Metals Handbook [8], initial loading of a virgin material typically produces more emission than subsequent loading. An "instantly-plastic" material will not produce any emission on later loadings, unless the previous load peak is exceeded or unless some type of deterioration occurred between loadings. This is the Kaiser effect. This behavior, for metallic materials, is due to AE generated by the acceleration/deceleration of large populations of dislocations under load. Hysteresis in these motions eventually leads to fracture. For composites, the discontinuities at the boundaries of different constituents (i.e., matrix and fibers) are much larger than the dislocations in metals. These discontinuities are stress raisers that contribute to degradation by development of distributed and distinctly different types of damage than metals. A typical damage progression scenario in a laminate composite is matrix microcracking, delaminations, disbonds, and finally fiber breakage. In the early stage of this progression, new surface is created internally without a significant loss in strength. However, as the specimen is strained, internal friction of these surfaces generates AE. If the geometry of the new surface developed at the peak strain is not completely locked in that configuration, it will emit AE at strains lower than the peak, when it is unloaded and reloaded. However, experience tells us that this typically is not indicative of intensive damage progression unless it occurs at a significantly lower fraction of the peak load or continues to occur during subsequent loading cycles. To paraphrase [8] again, structurally significant defects will tend to emit at loads below previous maximum, or, when the load is held constant. However, emission due to structure stabilization will tend not to recur. This is the Felicity effect and it is quantified by the Felicity ratio (FR): the load at which emission begins divided by the previous maximum load. The Kaiser effect is a FR of 1.0 or greater. For composite laminates, FR can systematically decrease under fatigue and FR less than 0.95 has been cause for rejection of FRP pressure vessels. [8]

One of the issues with evaluating material behavior according to the Kaiser effect and Felicity ratio is that existence of AE is affected by the signal amplitude. More specifically, the signal to noise ratio of a test configuration, as noted previously, governs trigger gains that one uses, which affects the size of signal that triggers event acquisition. Therefore when comparing the results of different tests one must be cognizant of all the factors affecting each test.

A zone location approach is used for this analysis by comparing cumulative energy arriving at different sensors. In other words, trends in cumulative energy at a sensor indicate proximity and intensity of damage. Event locations were calculated, and abandoned, because the complexity of the structure and the resultant anisotropy made the results hard to interpret. In addition, because a series of loading tests occurred, the behavior is assessed according to the Kaiser Effect.

4.0 Analysis

In the following discussion, AE events may be described as occurring at a particular sensor. This does not necessarily mean that the source of the AE event is right at the sensor indicated. It is shorthand for the scenario that the sensor is likely to be the sensor closest to the AE source. The stress wave propagation impinging on that sensor has the largest initial amplitude of all the waveforms monitored at all the sensors and therefore has triggered the data acquisition of that "event".

The panels were almost acoustically independent of each other for several reasons:

- Gaps between frames force acoustic coupling between frames from panel to panel via the bolted metal brackets. Optimum transfer across this joint is dependent upon matched acoustic impedances for all the components of the joint. This almost never happens to be the case. The presence of reflection and scattering surfaces from the bolt holes further tends to attenuate the transmission.
- Elastomeric sealants reduce acoustic coupling and dampen propagation.
- Bolted fabrication without adhesive (or with poorly bonded adhesive) reduces acoustic coupling.

Analysis of the sensor verification tests (pencil lead breaks, section 4.5) supported this concept. Signal loss was approximately an order of magnitude across a few feet of panel. Subsequently, the pressure test data was reduced by splitting the data into five panel files, each containing only the channels for each of the five panels. Filtering by energy threshold eliminated events occurring on other panels that were not registering on that panel. However, this does not eliminate any event that may register on another panel.

The most likely final failure sequence of the pressure cube, as noted in more detail elsewhere [3] is:

- Metallic frame splice failure: A frame splice cracked. These plates connected one section of the frame on the crown panel to another section of the frame on the adjacent rib panel. The particular splice in question is the one that connects the section of frame under AE sensors 27, 28, and 29 to the section of frame under AE sensors 22 and 23.
- Frame buckling: Once the splice plates failed, the detached rib frame of the speckled rib panel, subjected to increased in-plane bending, buckled.
- Integral cap failure: Post-frame-buckle load redistribution causes adjacent integral cap to fail.
- Catastrophic decompression in a fraction of a second: During this failure the cube rotated counterclockwise, as viewed from above. Sensors on the panel that blew out, were thrown up and out, as was the panel itself. This suggests that the panel failure initiated at

the left edge, air escaping to the left, quickly followed by detaching across the bottom and up the other side.

The following analysis attempts to map the damage development that led to this failure.

4.1 Checkout tests 1 and 2 (0.5P pressure where P=9.2 psi)

These two tests were performed to exercise all the COLTS testing equipment, systems, and test procedures. These tests were not expected to introduce any damage to the structure because the load of 0.5P was well below design pressure P. However, a few AE events did occur in both tests, but the amplitude was at least 2 orders of magnitude smaller than AE from later higher pressure tests. So, no intensive damage occurred, but some of these events possibly foretell the locations of the final failure.

During checkout test 1, only four AE events occurred, near the peak pressure, as seen in the "Load profile and AE Events" plot in figure 6. The load profile (vs. time in test) is the red trace and AE events are indicated by the blue dots. Three events occurred at sensor 16 on the bulkhead panel that did not fail, and one at sensor 31 in the center of the crown panel, between the regions later discovered to have delaminated. Please note, as seen in figure 7 of the waveforms captured at all the sensors for event 1, there does not seem to be much signal on the sensors other than 16, indicating a source very local to that sensor. However, after filtering out frequency content below 50 kHz, neighboring sensors 11, 14, 17, 18 do indicate some wave content other than noise. None of these sensors are near the panel that eventually failed but these events are either much smaller than the ones from the second checkout test or, as in the case of the channel 16 signal, are not particularly similar to that of a damage induced AE signal. Sensor 20 is showing a type of continuous AE not seen on the other sensors, although its frequency content (50-75 kHz) is much lower than the 400 kHz seen at sensor 16 and neighbors.

The high amplifier gains for this test highlight the larger noise amplitude at frequencies below 50 kHz on all sensors except 1, 13, 15 and 29. As noted previously sensors 1 and 13 are the only sensors mounted on a bay panel and may not have as much signal transmitted to them as the signal is carried on the stiffeners, hence the lower level of noise. All other sensors, as noted in Section 2, are opposite some internal structure such as a frame or stiffener. Channel (sensor) 15 failed and remained that way for the entire series of tests. Channel 29 showed weak signal for the entire test series despite troubleshooting prior to the failure test. The cause of the signal weakness for that channel was never ascertained because much sensor and cable damage occurred during the failure test.

During checkout test 2, only two AE events occurred, near the peak pressure, as seen in the "Load profile and AE events" plot in figure 8. These events show less localized (geographically) and longer (in time) activity, indicated by the number of sensors with significant waveform, as illustrated in figure 9 of event 1. The event registered significantly on sensors 19 to 26, as indicated by the red arrowhead line. These signals look more like typical damage-induced AE signals. Also, these sensors are on the speckle-pattern rib panel which suffered a metal splice fracture and frame buckling during later tests. Compared to the signals from checkout test 1, these signals are more likely to be from a distributed structural "damage" source. The response of event 2 is similar and has indications on sensors 1-6, 8, and 10. Note that sensors 1-6 are on

the panel that eventually blew out entirely during the failure test. Sensors 8 and 10, albeit on another panel, are closest to the edge contiguous to the "failure" panel.

In summary: AE signals from these "checkout" tests are much smaller than failure events occurring in later tests, but the general locations of sensors showing AE-like indications are consistent with the location of the final catastrophic failures of the speckled rib and bulkhead panels. This shows potential for vehicle health monitoring by damage "precursor" AE.

4.2 Test 3: 1P pressure

The load profile and AE event plot for the 1P test is shown in figure 10. The dotted green lines indicate the point in time where the pressure reaches the previous peak pressure achieved during the 0.5P tests. A Felicity Ratio of 1 indicates that no structurally destabilizing damage occurred during the 0.5 P tests The black vertical line indicates the beginning of the unloading. Events after this point indicate that some damage, which created new surface, had occurred during this test. As the load reduces, the friction of these surfaces coming together creates acoustic emission as they interfere.

For this analysis, the cumulative energy of the events was calculated for each channel (sensor) and is plotted, versus time, for each panel as seen in figures 11-15. Red ovals indicate items of interest. In figure 11, the speckled bulkhead panel that blew-out during the failure test, has a significant rapid coordinated jump in energy occurring on all sensors around 1680 seconds (~ 8.6 psi). Sensor 1 with the lowest cumulative energy is bay-located. This bulkhead panel had the next-to-the-highest cumulative energies per sensor. Figure 12 shows the cumulative energy plot for the gray rib panel, which is opposite the failure initiating speckled rib panel. It has the lowest sensor energies of all the panels. Now, note that the cumulative energies of the gray bulkhead panel, as seen in figure 13, includes the highest energies, with the largest increases occurring at 1790 seconds right before unloading. This panel is farthest from the later failure locations, so hindsight allows us to suggest that these events were "structurally stabilizing" because their location is not involved in the final failure. However, they did occur on a bulkhead panel, suggesting that these types of panels may be more likely to fail and should be monitored more closely. Significant coordinated increases also occur on most sensors of that panel at 1610 seconds (~ 8.0 psi) and 1660 seconds (~ 8.5 psi), especially sensors closer to the floor (16, 17, and 18). The smallest increases occurred at sensor 13 (bay-located), and 15 (failed). Figure 14 shows a significant coordinated increase at 1720 seconds (~ 9.0 psi) of the cumulative energies of the speckled rib panel which later had initiated the final catastrophic failure. It also has the next lowest cumulative energies of the side panels. Comparable cumulative energies are noted for the crown panel as seen in figure 15. There is a coordinated increase around 1650 seconds (~ 8.4 psi) with sensor 27 having the greatest increase by 1700 seconds. Sensor 27 is closest to the metal splice failure on the affected frame. The greatest total cumulative energy occurs on sensor 31. After the 2P test, delaminations were discovered that run along the edges of the crown panel contiguous to the rib panels. Sensors 31 and 28 are closer to both of those edges than the other crown sensors. An explanation for the large total cumulative energy at 31 may be that the delamination damage (or delamination-initiating damage) was already occurring near both sensors 30 and 32. Although the energy at sensor 30 or 32 would be greatest from the damage nearest to each, the sum of the energy from both damage regions could be greater at the sensor in the middle, 31. This may also account for the higher total cumulative energy (vs. others on same

panel) at sensors 20 and 9 on the rib panels (adjacent to 30 and 32 respectively). In figure 14, sensor 20 obviously leads the others on the speckled rib panel. In figure 12 it is harder to see, but 9 is at the top with 10 and 11 by the end of the test.

In summary, the highest cumulative energies occurred at symmetric locations: the speckled bulkhead panel (that eventually failed) and gray bulkhead panel. The lowest energies (not counting the crown) occurred on the two rib panels. This leads one to surmise that even though the bulkhead panels have one more stiffening stringer than the rib panels, something about the construction of the bulkhead panels contributes more to damage development. As seen in all the figures 11-15 the existence of events during unloading indicates that some significant damage had occurred during this test. Assuming that the coordinated increases in cumulative energy are indicative of primary damage mechanisms the chronology of damage development is as follows:

- 1610 seconds (~ 8.4 psi) Bulkhead, gray: near bottom of panel
- 1650 seconds (~ 8.4 psi) Crown: front left (as if facing speckled bulkhead)
- 1660 seconds (~ 8.5 psi) Bulkhead gray: near bottom of panel
- 1680 seconds (~ 8.6 psi) Bulkhead speckled: left
- 1720 seconds (~ 9.0 psi) Rib speckled: all
- 1790 seconds (~ 9.2 psi) Bulkhead gray: lower left

Also, evidence suggests that the later-discovered crown panel delaminations were already in development during this test.

4.3 Test 4: 2P pressure

The load profile and AE event plot for the 2P test is shown in figure 16. Some randomness was seen in the test pressure values (red dots), so a smoothed version was calculated and is plotted as the black curve. The dotted green lines indicate the point in time where the pressure reaches the previous peak pressure achieved during the 1P tests. A Felicity Ratio of approximately 0.3 supports the conclusion that significant damage did occur during the 1P test. Since the trigger gain was reduced 3 dB from the 1P test to the 2P test, this FR is especially indicting because AE may have been sensed even earlier if the higher gain had been used. The overall larger number of events during 2P test compared to 1P test indicates more rapid damage progression. The larger number of events during unloading after 1100 seconds (~ 20 psi), than has occurred during previous unloadings, also indicates more significant damage had occurred during the 2P test than previously. Figure 17 is a closer view of the same data with a region of interest shaded in yellow between 16-18 psi (885-950 sec) indicated because of increasing strain gauge activity at that time.

As indicated by the red arrow on the cumulative energy plots for all the panels (figures 18-22), all sensors show significant rate increase in cumulative energy around 1060 seconds (~ 19 psi). The vertical black lines indicate the beginning of unloading. In figure 21 of the speckled rib panel that initiated failure during the failure test, a significant increase occurred during unloading; suggesting that the metallic frame splice failure began during the 2P test. Figures 23-27 are close-ups of the cumulative energy plots with the yellow shaded region of strain gage activity-increase between 16 and 18 psi. The red ovals highlight significant increases in cumulative energy, most of them occurring well before the strain gages indicated damage.

During the 16-18 psi window, higher rates of increase (excluding the noted jumps) in the cumulative energy, occurred on the speckled bulkhead panel (figure 23) and the speckled rib panel (figure 26). Also, on all the panels except the gray bulkhead panel, around 18 psi (950 seconds) at the end of the yellow shaded region, more rapid increases in cumulative energy occurred, especially on speckled rib and crown panels (noted for the delaminations that were discovered after this test). The largest cumulative energy at that point (around 1000 seconds, still approximately 18 psi) are on the speckled rib panel followed by the speckled bulkhead. Sensors 19 and 20 leading on the speckled rib panel may be due to delamination growth in the crown away from sensor 30 toward 27. On the crown, sensor 27 lead with highest cumulative energy for most of the test, followed by sensors 28 and 31. Sensor 27 is the closest crown sensor to the metal frame splice that had failed, suggesting damage development that lead to the splice failing. Both sensors 28 and 31 being high indicate that both delaminations in the crown were growing. As noted previously sensor 29 was weak during the entire series of tests.

All the noted indications suggest that the critical damage on the "failure initiation" panel (speckled rib) and the "blow-out" panel (speckled bulkhead) was already occurring and that structural integrity and remaining fatigue life had been severely compromised.

Summary:
The highest accumulated energies are from the speckled rib panel, followed by the speckled bulkhead panel.

Chronology of indications:

- 820 seconds (~14 psi): Rib speckled, Ch. 19, 21, 22, 23, 24 rate increases (mid to upper right around impact)
- 820 seconds (~14 psi): Crown, Ch. 27, 30, 31, (left edge around back left corner, if facing bulkhead speckled)
- 835 seconds (~15 psi): Bulkhead speckled, Ch. 2-6 especially 3 and 5
- 835 seconds (~15 psi): Rib gray, Ch. 8, 10-12 especially 10 and 12 (lower right corner)
- 800-840 seconds (~13.5-15 psi): Bulkhead gray, no jumps but energy rate Ch. 16-18 increasing past Ch 14 (bottom).
- 875 seconds (~15.5 psi): Rib speckled, Large energy release especially Ch 25 (bottom).
- 940 seconds (~16.5 psi): Rib gray and Rib VIC
- 950 seconds (~18 psi): Rib speckled, all and crown all except 29 and 32
- 950 seconds to end of test: rate increases at most all sensors, again especially on the speckled rib panel followed by the speckled bulkhead panel.

4.4 Test 5: Failure

The load profile and AE event plot for the failure test is shown in figure 28. The dotted green lines indicate the points in time when AE starts and the time when the pressure reaches the previous peak pressure achieved during the 2P tests. A Felicity Ratio of approximately 0.6 indicates that more damage did occur during the previous 2P test Failure occurs a little after 2000 seconds at a pressure of approximately 48 psi (approximately 5 times the design pressure P=9.2 psi). Figures 29-33 are the cumulative energy plots. All of the plots show a leveling off or reduction of AE rate around 1550-1600 seconds, which coincides with a pressure hold of approximately a minute. This illustrates the extent that AE event rate is affected by load rate.

Variations in load rate should be kept to a minimum during testing, especially when analyzing the AE for onset of different failure mechanisms. The overall behavior, more obvious in this test, but also occurring during previous tests, is that the sensors nearer the floor (especially 6, 12, 18) tend to lead in cumulative energy for each side panel. This could be due to the hatch or the different construction of the floor (relative to the other panels) either making more noise or increasing stresses at the edge of the other panels.

The raw average AE data rate was much higher for this test than for the previous 2P test:

- 2P: 8209 events over 1300 sec = 6.3 event/sec
- Failure: 50001events over 2000 sec = 25 events/sec (approx. 4X higher)

Because of the increased AE rates, even after filtering, there does not seem to be many easily identified jumps in cumulative energy for this test as opposed to previous tests. This suggests a new regime of damage development. Previous tests had large events followed by periods that were more quiescent. In those tests, stress redistribution after stress relief allowed structural stability for a period of time before stress buildup exceeded local weakness. In this test, large and small events are more evenly distributed in time and location. Dynamic load redistribution almost immediately causes more damage. Failure is accelerating.

Some sense of failure progression can be illustrated by tracking increases of cumulative energy rates. The activity on the right side of the speckled bulkhead (sensors 3 and 5) panel picks up around 1700 seconds (~38 psi) compared to the left side. The rates during the pressure hold, around 1600 sec (~ 36 psi), do not flatten as much as in the other panels. This suggests the panel is weaker or the stresses higher than the other panels, especially since there was also a short pressure hold at 1700 seconds. The entire gray rib panel also seems to be ramping up about the same time with sensors 10-12 (on the lower half) leading. Both the gray rib panel and gray bulkhead panel are more quiescent than the other panels, relatively speaking, if not including the near-floor sensors. Looking at the speckled rib panel where the frame buckled, four sensors were located equidistant from the prescribed impact on the integral cap: 21, 22, 23, and 24. We see a distinct increase at sensors 22 and 23 (located on that frame) at 1840 seconds (~ 41 psi) but not at sensors, 24 and 21, which are near the integral cap. Expecting the impact to have a consistent effect on the damage development and hence AE received at all four sensors, 21-24, the increase suggests that this is when either the frame metal splices started cracking and/or the frame was weakening. As to the question of whether the impact had any effect at all on initiating the failure, one should note that earlier, between 1400 and 1500 seconds (28-32 psi) the sensors around the impact (21-24) are starting to lead the others (not including the floor sensor 25). This is not definitive evidence, but it raises the possibility that the impact contributed to local weakening. This could have led to the frame or frame/panel interface weakening before the splice failure. For the crown, the central edge sensors (28 and 31) have highest cumulative energy. These sensors are closest to *both* of the crown delaminations, which already existed before this test, as noted previously. This suggests that the delaminations are either growing or rubbing to create AE.

Summary:
Damage Chronology

- ~20 psi (1200 sec): Cumulative energy at bottom of gray bulkhead leads others.
- ~24 psi (1300 sec): Cumulative energy of other bottom sensors (6, 12, 25) also leading.

- ~32 psi (1550-1600 seconds): Most all sensor energies start to level off due to pressure hold, except for the sensors of the two bulkhead.
- ~38 psi (1700 sec): Most all sensor energies ramping up again, even though there was another pressure hold at 1700 seconds.
- ~41 psi (1840 sec): Energy increase beginning on frame that buckled at sensors 22 and 23.

4.5 Pencil lead breaks: Pre-test and Post 2P

The pencil lead break (PLB) is a standardized method [9] for testing AE sensor and instrumentation response. It consists of loading a graphite pencil lead in bending at a particular angle to a surface (governed by the addition of a guide ring to a mechanical pencil) as illustrated in figure 34. When the lead breaks, a step-unload of the surface generates stress waves propagating in the structure away from the point of loading. Figure 35 shows the resultant load traces of 10 PLB's overlaid to illustrate the repeatability of the step unload [7]. The peak loads at breakage (notation 2) are within approximately ± 8% of -0.75 N (-0.17 lb) illustrating that it is reasonably consistent. One can also see that the load rate of the lead on the surface (notation 1) is much slower than the unload. The resultant wideband AE is more of a function of the response of the material, as illustrated by the reverberation of the load cell (notation 3) used to measure the PLB's, than the application of the load. This is much more analogous to the stress release of damage development in the material than the classic coin tap test (and later variants) where the impact of the coin governs the response. In plate-like structures, the resultant AE plate wave propagation is very similar to that generated by microstructural damage development.

For the PRSEUS pressure cube, tests two series of PLB's with the same data acquisition settings were executed: one series prior to any pressurization tests at Langley and one after the 2P test, but before the final failure test. The PLB's were performed adjacent to every AE sensor. Data acquisition is the same as in a regular AE test such that wave propagation arriving at all the sensors was captured for each PLB at a single sensor. Prior to the failure test, the cube had to be tipped on its side to apply a damage initiating impact. Sensors 1 and 14 had been dislodged and reattached, hence, initiating the second series of PLB's. The original intent of the PLB's was only to check out the sensor attachment and instrumentation, so no particular care was taken to conduct the PLB's in exactly the same locations for each series. However, they were conducted approximately an inch away from each sensor in the same manner as noted in the standard.

The energy propagating to distant sensors is less likely to be affected by local variations in PLB location than by the types of damaged structure the wave propagation would have to traverse. Distributed damage that occurs early in the damage progression of composites tends to attenuate signal strength so typically energy received at a sensor would be expected to be lower post-damage.

Two scenarios could explain the inverse behavior of energy being higher post-damage. There is an increased potential for unstable residual stresses, due to load cycling, that could release and add to the stress wave when tripped by that passing wave energy. Also, the cube is a combination of different geometries and local stiffness. In the virgin condition, the stress wave propagation away from a PLB has a particular distribution due to these variations. This distribution will be

affected, with damage localization, as many smaller cracks coalescence into larger discontinuities, possibly focusing the energy at some sensors. In particular, damage along the stiffener/panel interface could reduce the transfer of wave propagation into the stiffener, thereby increasing the amplitude at the sensor, given everything else equal.

For these tests, an indication of the energies collected at all sensors due to one PLB is made by calculating the RMS (root-mean-square) value for each collected waveform. This is plotted in figures 36-37 with respect to each sensor. Figure 36, for a PLB at sensor 13, shows the expected behavior of attenuation from damage development because all the RMS values prior to testing (blue X) are higher than after the 2P test (red X). To accentuate the sometimes small differences in RMS value, the scale for RMS is such that the values collected at the PLB sensor are off the graph. Figure 37 illustrates the opposite behavior where the post test RMS values are larger than the pretest. Figures 38-41 are spectra of the waveforms collected at a PLB sensor and its nearest neighbors. The pre-test to post comparison of spectra of the "expected-behavior" responses, seen in figures 38 and 39, respectively, shows a decrease in energy post-2P across most all frequencies. Figures 40 and 41, illustrating the inverse behavior for the PLB at sensor 1, show the increase occurring predominantly in the frequencies below 150 kHz. Note that sensor 1 is on the panel that blew out during failure.

Therefore, comparing the number of times sensors had signal energy increased (i.e. more energy received post-2P than before testing) and tabulating by panel we have the following results:

- Bulkhead (VIC, failed) 34
- Rib (VIC, impacted) 10
- Crown 9
- Bulkhead (gray) 6
- Rib (gray) 4

Note the interesting correspondence of behavior with damage. The bulkhead panel that blew out had the most "increased energy" behavior and the rib panel that initiated failure had the second most. In third is the crown panel, which had major delaminations.

Summary:

- The locations of the sensors with "increasing" energy PLB behavior seem consistent with major structural failures of the speckled rib and bulkhead.
- PLB response may be useful as an indicator of structural damage on a large scale.
- Identification of particular frequency bands that may be more sensitive to damage merits further investigation.

5.0 Lessons Learned, Summary, and Conclusions

Lessons Learned:

- The AE event rate is affected by load rate. Variations in load rate should be kept to a minimum during testing, especially when trying to analyze the AE for onset of different failure mechanisms.

Summary and Conclusions:

- The AE signals from the 0.5P "checkout" tests are much smaller than events occurring in later tests, but the locations of sensors showing AE-like indications are generally consistent with the location of the final catastrophic failures of the speckled rib and bulkhead panels.
- In the 1P test, the highest cumulative energies occurred at symmetric locations: the speckled bulkhead panel (that eventually failed) and the gray bulkhead panel. The lowest energies (not counting the crown) occurred on the two rib panels. This leads one to surmise that even though the bulkhead panels have one more stiffening stringer than the rib panels, something about the construction of the bulkhead panels contributes more to damage development. A Felicity Ratio of 1 indicates that no structurally destabilizing damage occurred during the 0.5 P tests. However, the existence of events during unloading indicates that some significant damage had occurred during the 1P test. Also, evidence suggests that the later-discovered crown panel delaminations were already in development during this test.
- For the 2P test, in general, a Felicity Ratio of approximately 0.3 supports the conclusion that significant damage did occur during the 1P test. The larger number of events during unloading, than had occurred during previous unloadings, indicates more significant damage had occurred during the 2P test than previously. All indications suggest that critical damage on the "failure initiation" panel (speckled rib), metal frame splice, and the "blow-out" panel (speckled bulkhead) was occurring. Crown panel delaminations were growing.
- For the Failure test, again, a Felicity Ratio of approximately 0.6 indicates that more damage did occur during the previous 2P test. The crown delaminations are continuing to emit AE. Indications raise the possibility that the prescribed impact contributed to damage which led to the frame weakening preceding the splice failure.
- PLB's & AE in early tests ("precursor" AE): These types of tests may indicate the appropriate regions that will ultimately fail. Closely monitoring those regions may prove to be an efficient and effective means of structural health evaluation.

6.0 References

[1] Vicroy, D.D. Jegley D.C., Cosentino G. “NASA Blended-Wing-Body Research Overview”. 67th Annual International Conference on Mass Properties Engineering. Seattle, Washington 2008

[2] Velicki, A. “Damage Arresting Composites for Shaped Vehicles,” NASA CR-2009-215932, Sept. 2009.

[3] Yovanof, N.P., and Lovejoy, A.E.,.Baraja, J., Gould, K, "Design, Analysis and Testing of a PRSEUS Pressure Cube to Investigate Assembly Joints," 2012 Aircraft Airworthiness and Sustainment Conference, April 3, 2012, Baltimore, MD.

[4] Yovanof, N.P. et al, “Pressure Cube Test Specification” Boeing Research and Technology, Document ZA153690, 2011

[5] Sutton, M., Cheng, M., Peters, W., Chao, Y., and McNeill, S.,“Application of an Optimized Digital Correlation Method to Planar Analysis,” Image and Vision Computing, Vol. 4, No. 3, 1986, pp. 143–151. doi:10.1016/0262-8856(86)90057-0

[6] Schreier, H., Braasch, J., and Sutton, M., “Systematic Errors in Digital Image Correlation Caused by Intensity Interpolation,” Optical Engineering, Vol. 39, No. 11, 2000, pp. 2915–2921. doi:10.1117/1.1314593

[7] Horne, M. R. “Rayleigh Wave Acoustic Emission during Crack Propagation in Steel”. PhD Dissertation, Virginia Polytechnic Institute and State University. 2003.

[8] ASM handbook Vol. 17 Nondestructive Evaluation and Quality Control: Acoustic Emission Inspection.

[9] ASTM E976 "Standard Guide for Determining the Reproducibility of Acoustic Emission Sensor Response“

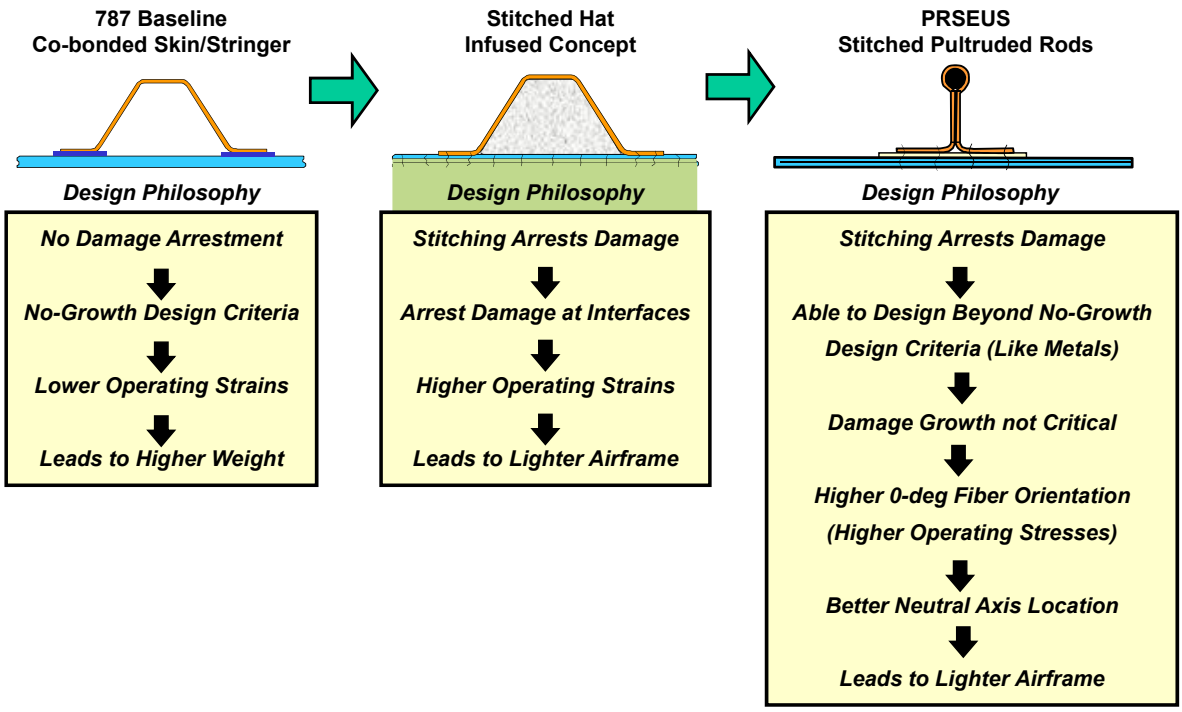

Figure 1. Evolution of BWB fuselage design [1]

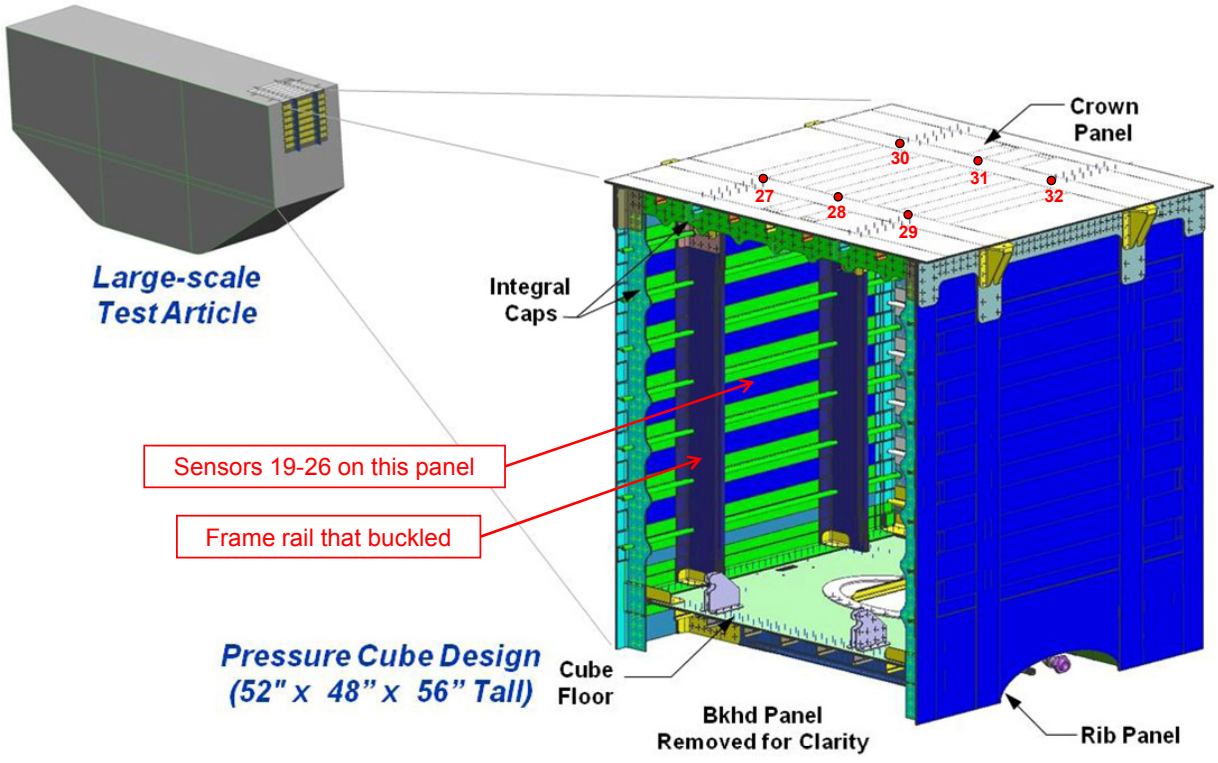

Figure 2. Schematic of Pressure cube with approximate locations of some of the AE sensors (red dots) mounted on the crown panel and other notations in red by the author. [4]

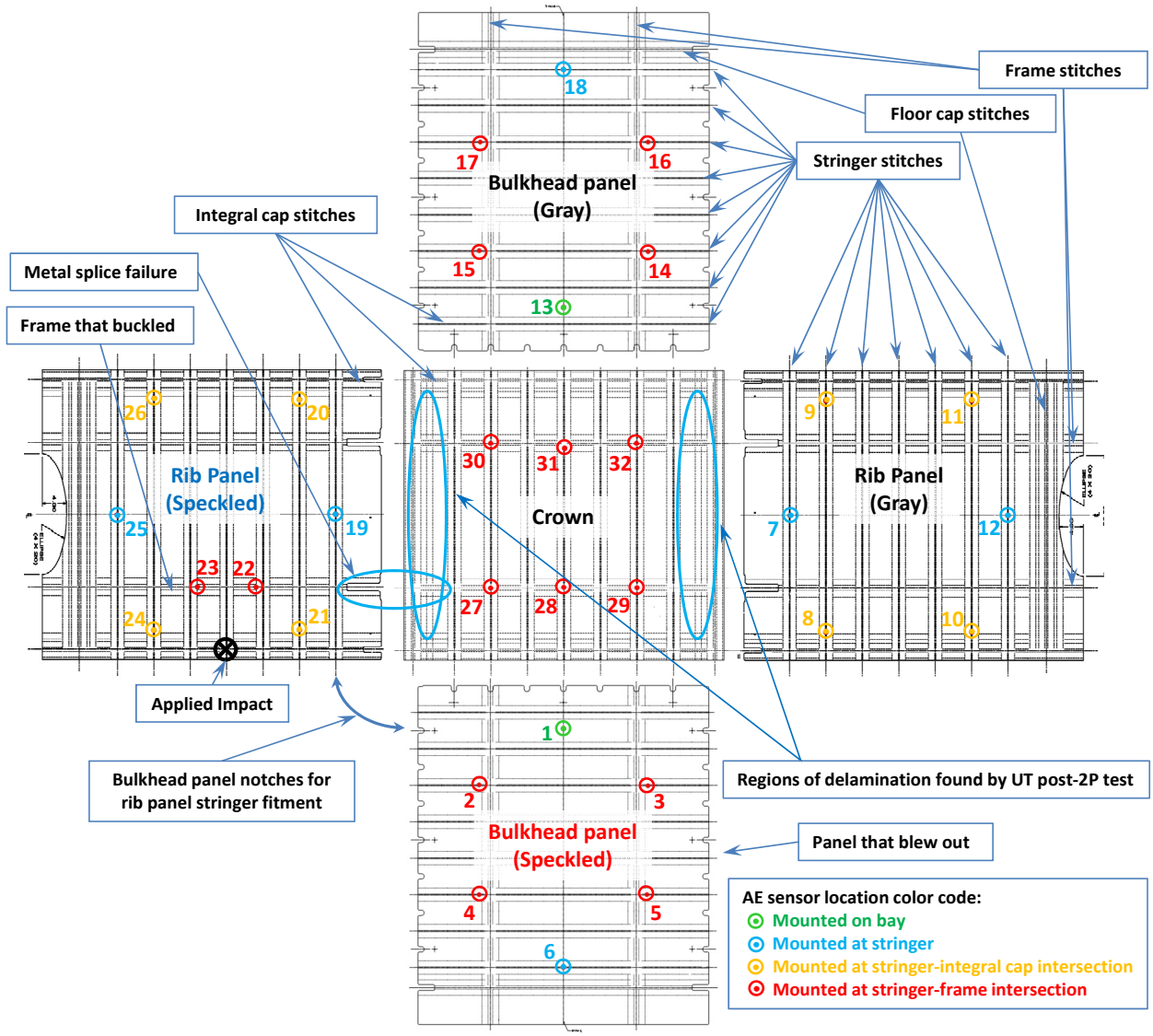

Figure 3. Locations of AE sensors on the panels of the pressure cube

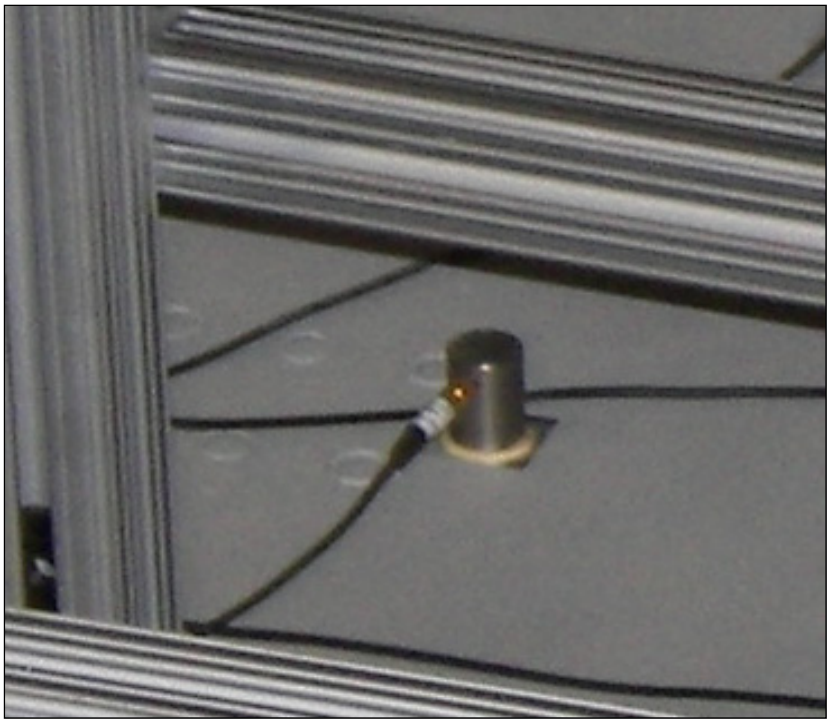

Figure 4. Installation of one AE sensor on the crown panel

Test		Signal		Trigger		Data Acquisition (Sampling)				Parametric (Sampling)	
Description [and ID]	Date	Gain (dB)	HP Filter (kHz)	Gain (dB)	BP Filter (kHz)	Rate (MhZ)	Range (V)	Points	Pretrig	Rate (Hz)	Range (V)
Pencil lead breaks to check AE channels	7/29/2011	24	20	21	50 - 750	1	+/- 1	2048	256		
Pneumatic pressure 0.5P (P = 9.2 psi) [Checkout 1]	7/29/2011	48	20	33	50 - 750	1	+/- 1	2048	256	0.5-1*	+/- 10
Pneumatic pressure 0.5P [Checkout 2]	7/29/2011	48	20	33	50 - 750	1	+/- 1	4096	256	0.5-1*	+/- 10
Pneumatic pressure 1P [Shaker 1P]	7/29/2011	48	20	33	50 - 750	1	+/- 1	4096	256	0.5-1*	+/- 10
Pneumatic pressure 2P [Pressure 2P]	7/29/2011	36	20	30	50 - 750	1	+/- 1	4096	256	0.5-1*	+/- 10
Post-“applied impact” PLB’s	8/9/2011	24	20	21	50 - 750	1	+/- 1	2048	256		
Failure @ 48 psi [Pressure failure]	8/10/2011	24	20	30	50 - 750	1	+/- 1	4096	256	0.5-1*	+/- 10

Figure 5. AE Instrumentation Settings

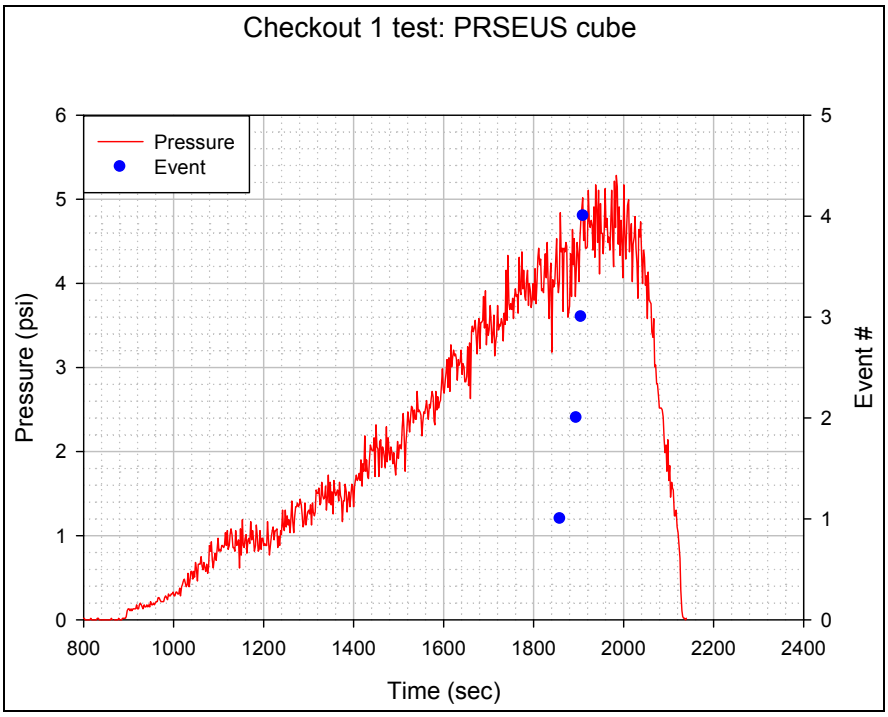

Figure 6. Checkout test 1 (0.5P, P=9.2 psi) Load profile and AE events

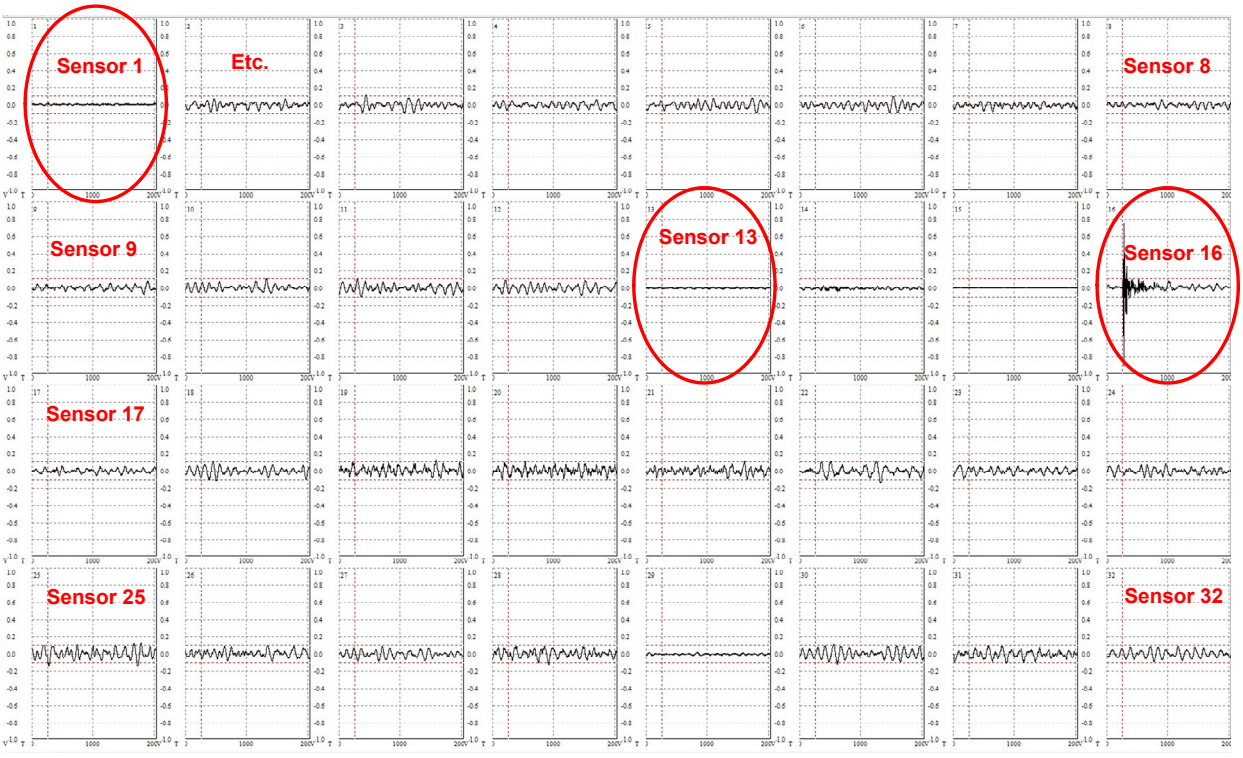

Figure 7. Checkout test 1 waveforms from AE event #1 captured at all the sensors

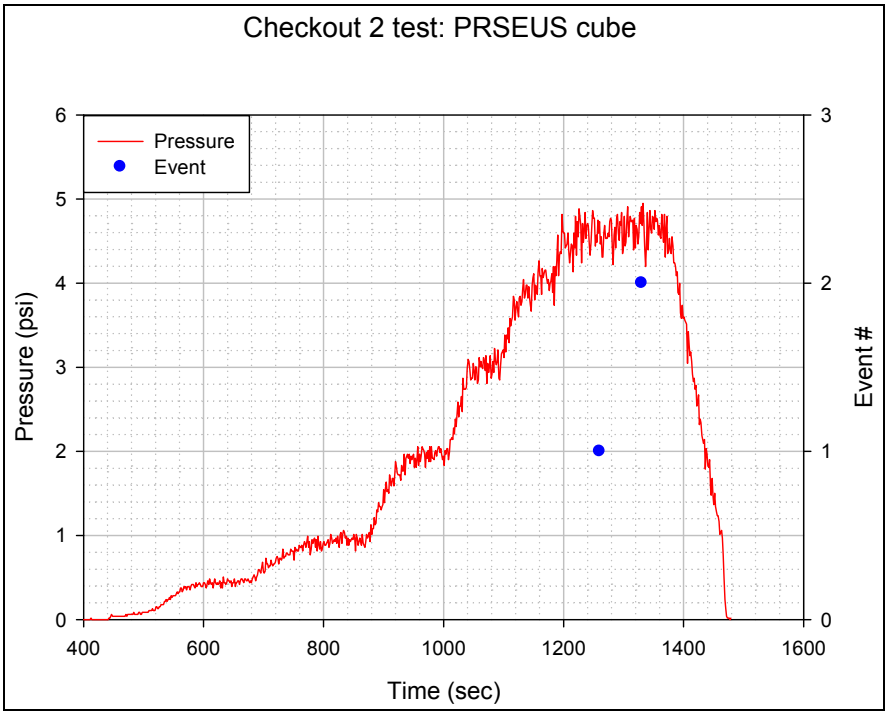

Figure 8. Checkout test 2 (0.5P) Load profile and AE events

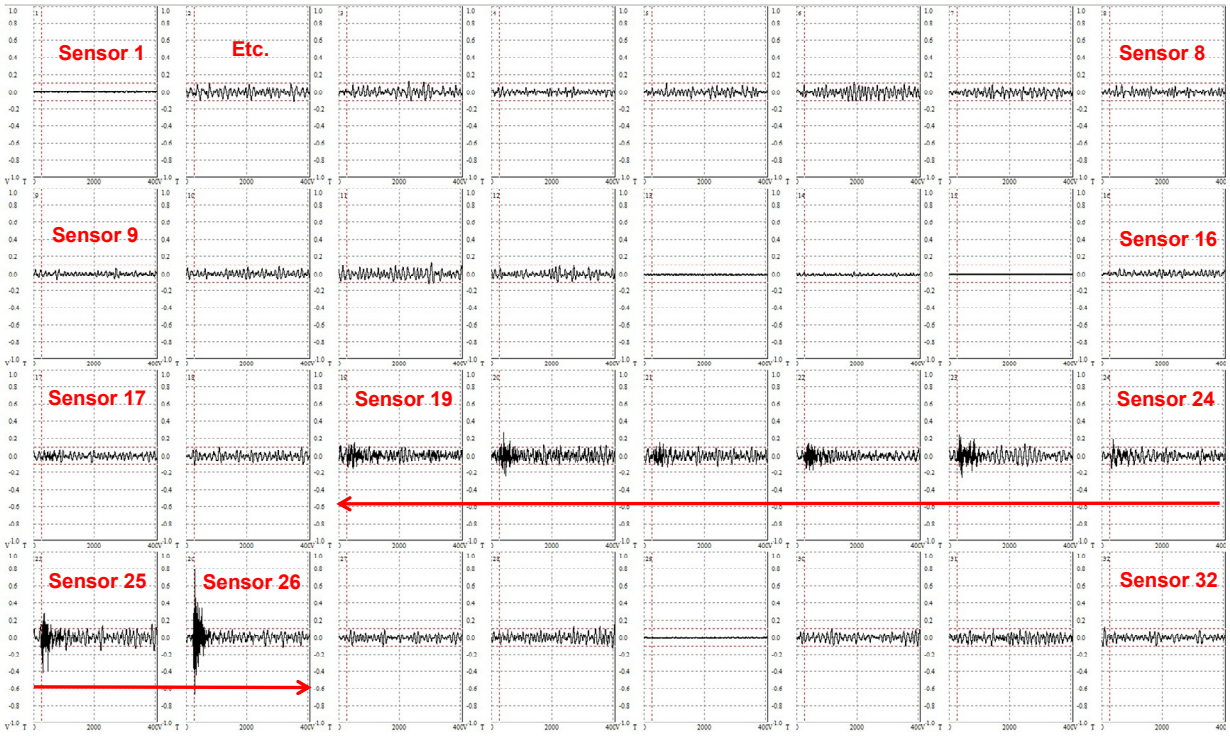

Figure 9. Checkout test 2 waveforms from AE event #1 captured at all the sensors

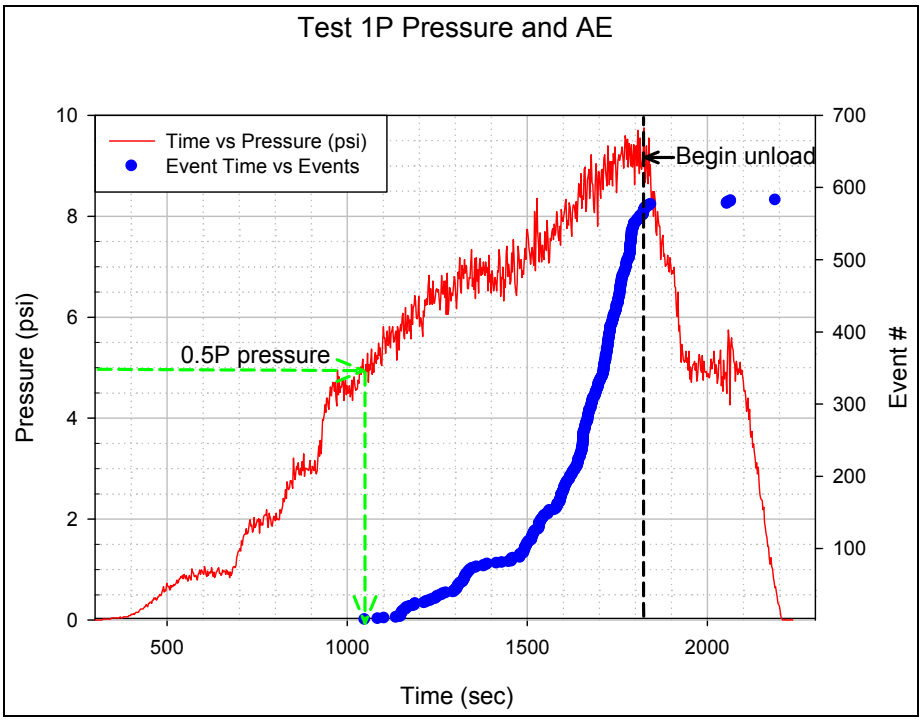

Figure 10. Pressure 1P Test Load profile and AE events

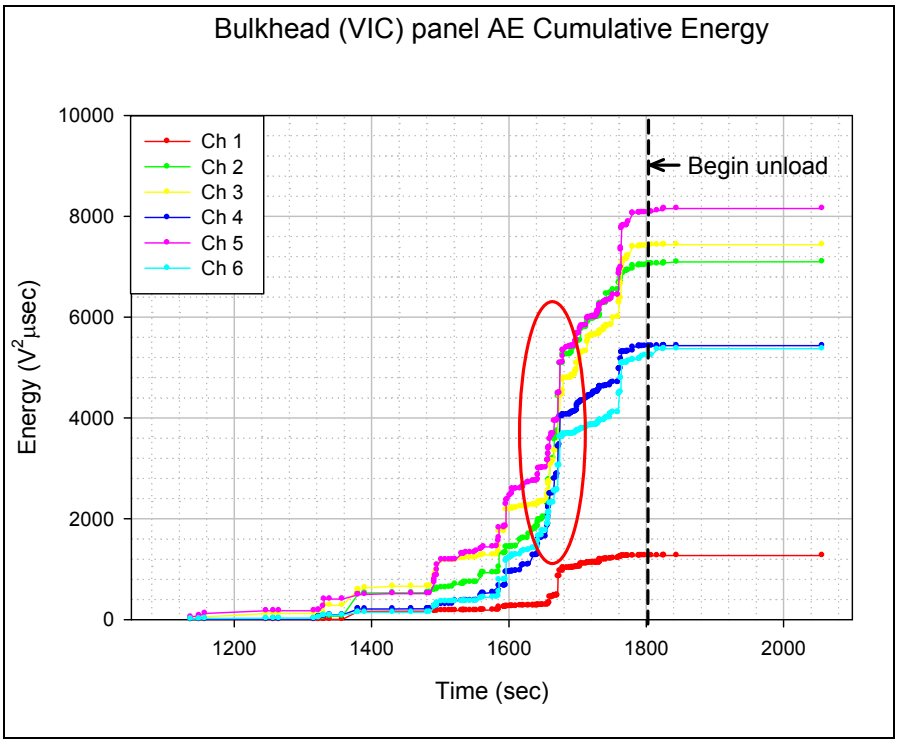

Figure 11. Pressure 1P Test: Speckled bulkhead panel AE energy

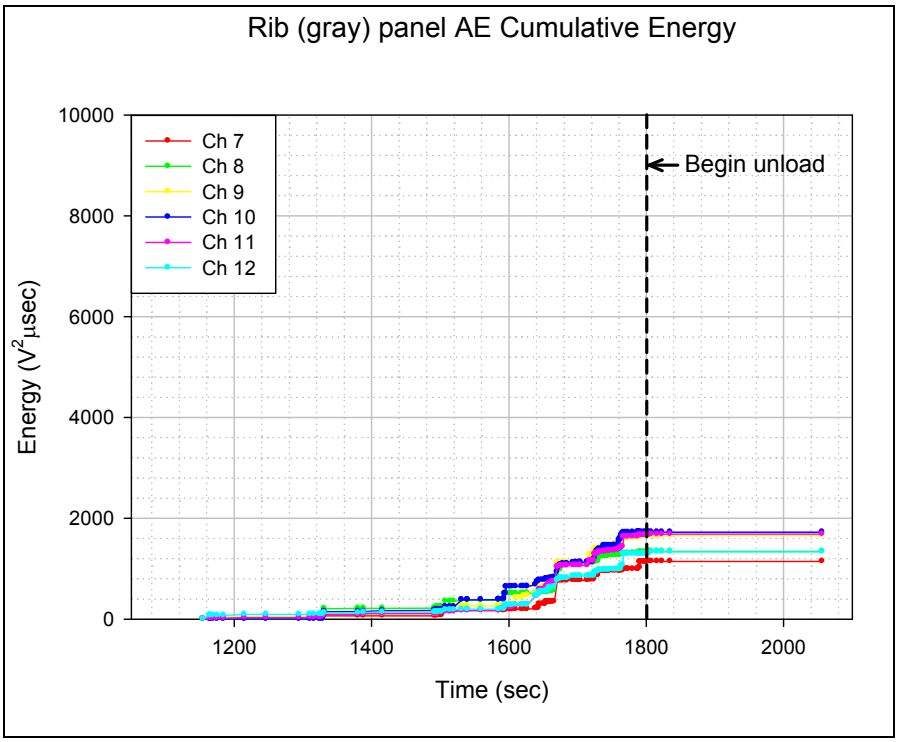

Figure 12. Pressure 1P Test: Gray rib panel AE energy

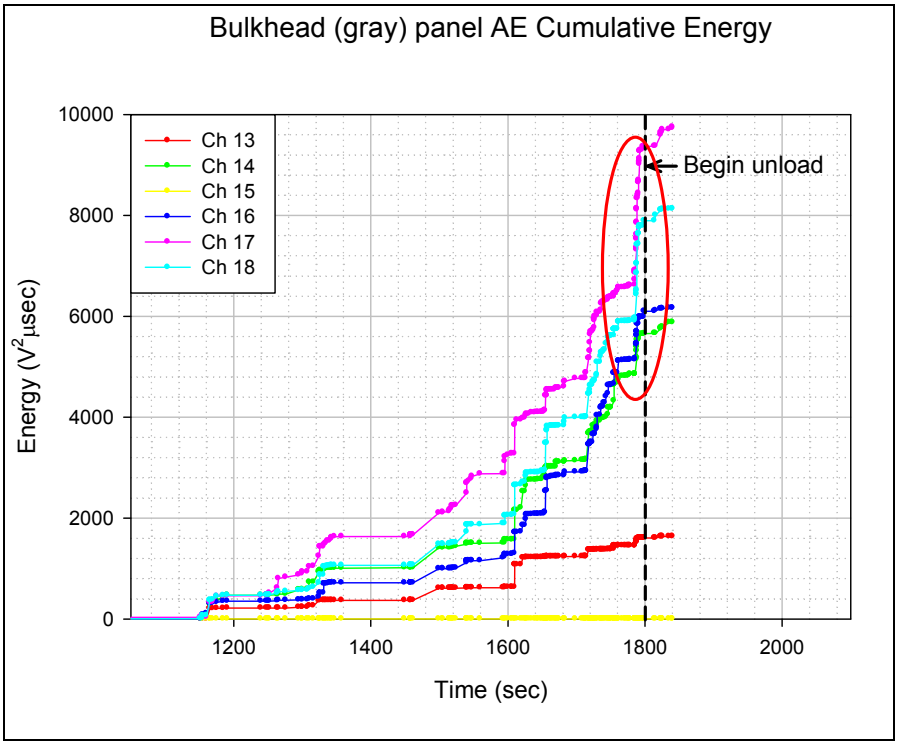

Figure 13. Pressure 1P Test: Gray bulkhead panel AE energy

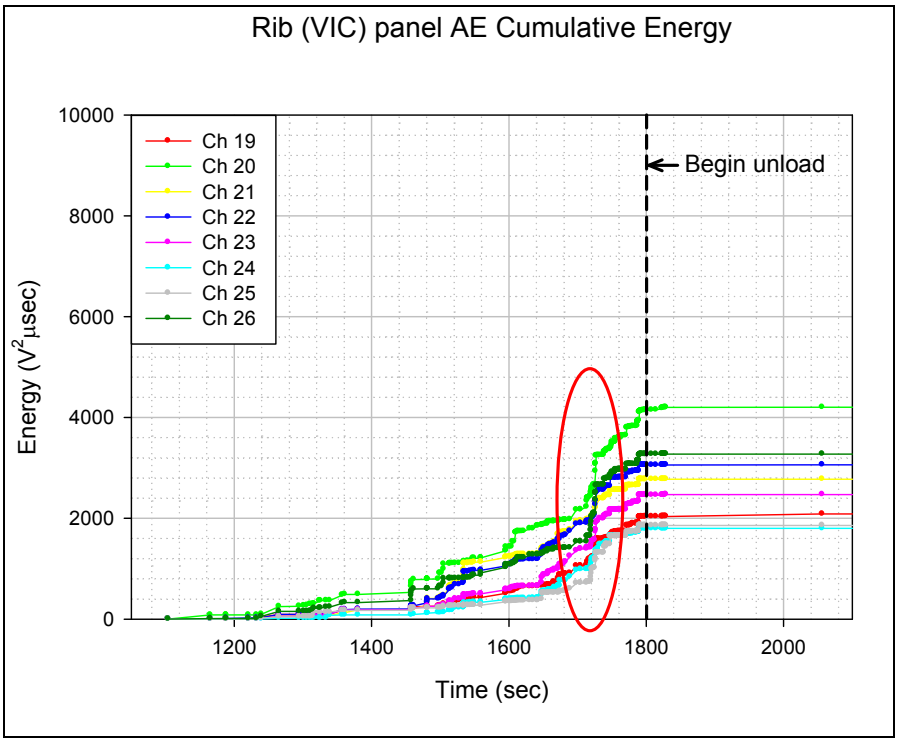

Figure 14. Pressure 1P Test: Speckled rib panel AE energy

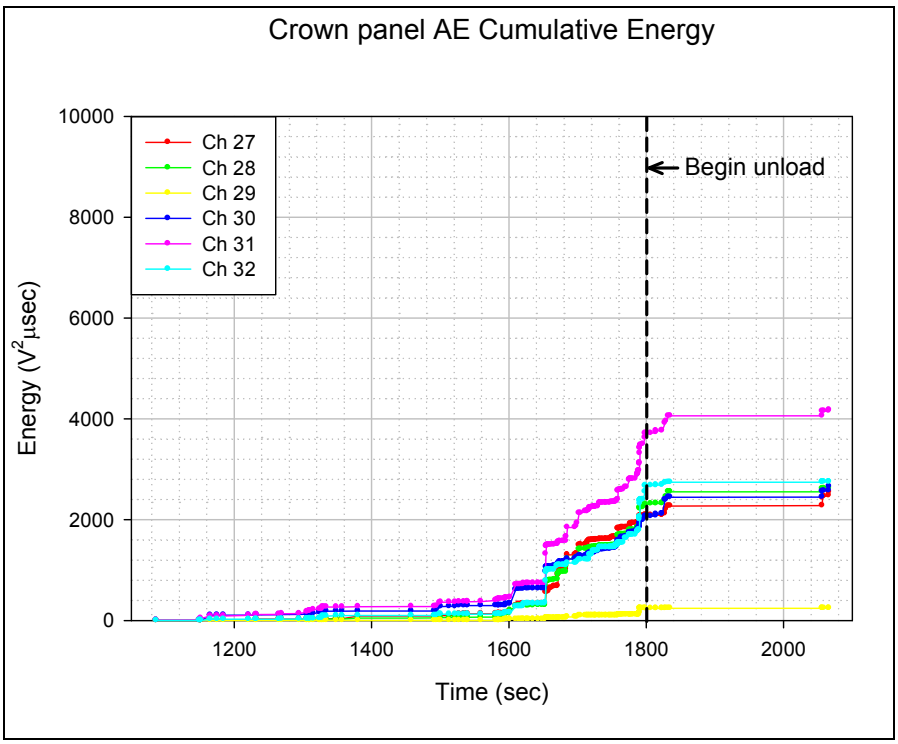

Figure 15. Pressure 1P Test: Crown panel AE energy

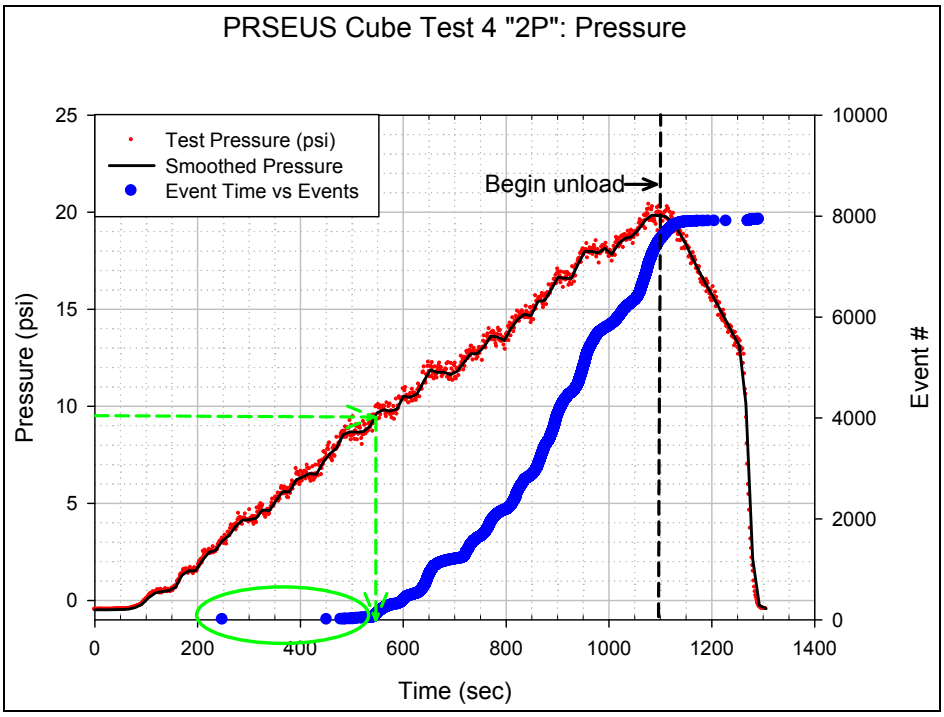

Figure 16. Pressure 2P Test Load profile and AE events

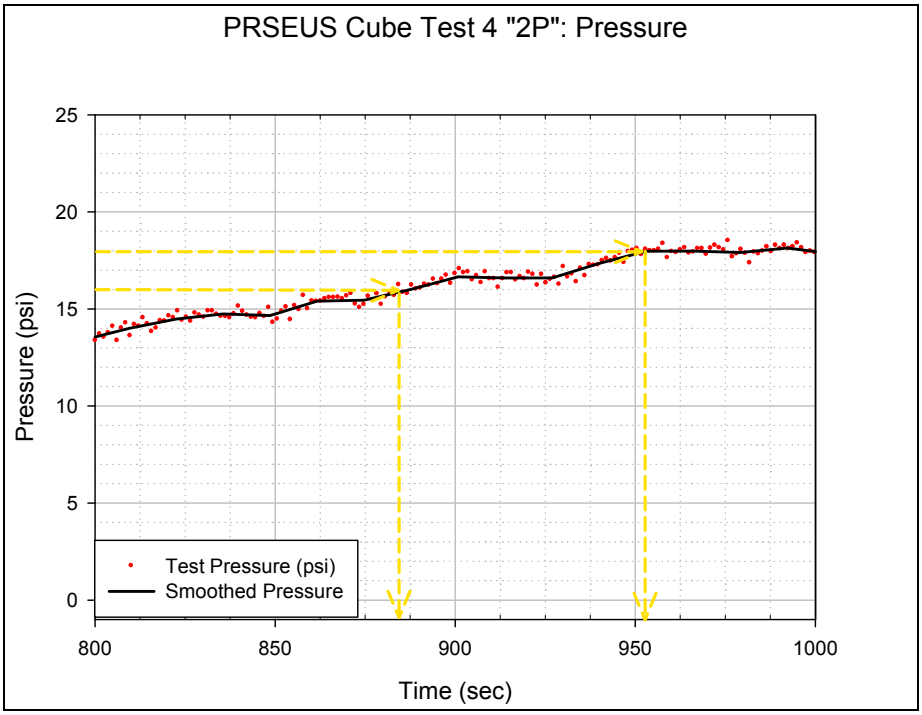

Figure 17. Pressure 2P Window of increasing strain gage activity

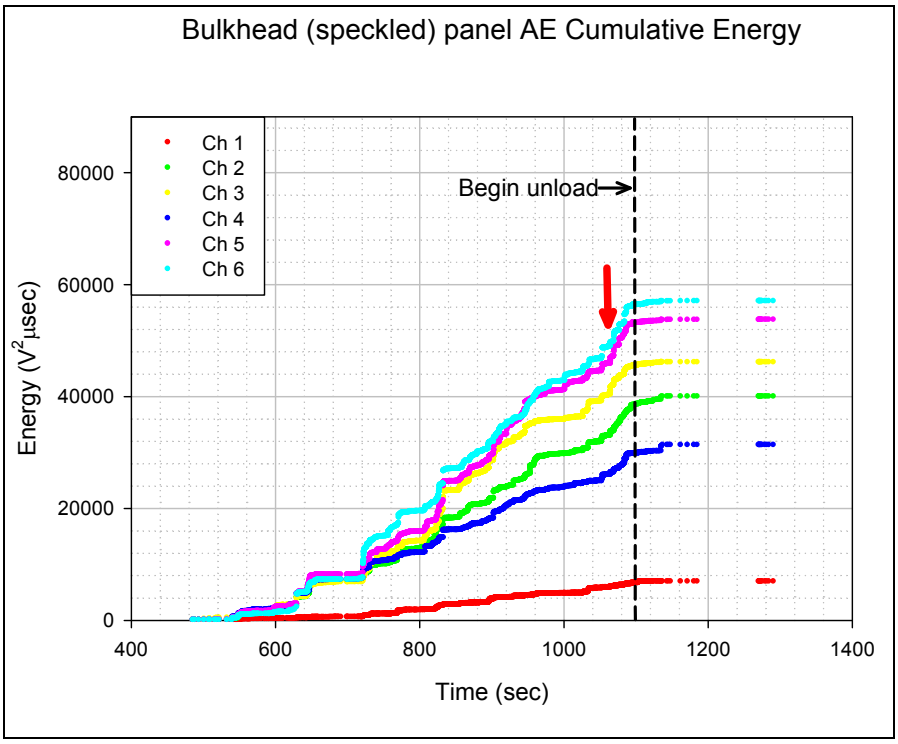

Figure 18. Pressure 2P Test: Speckled bulkhead panel AE energy

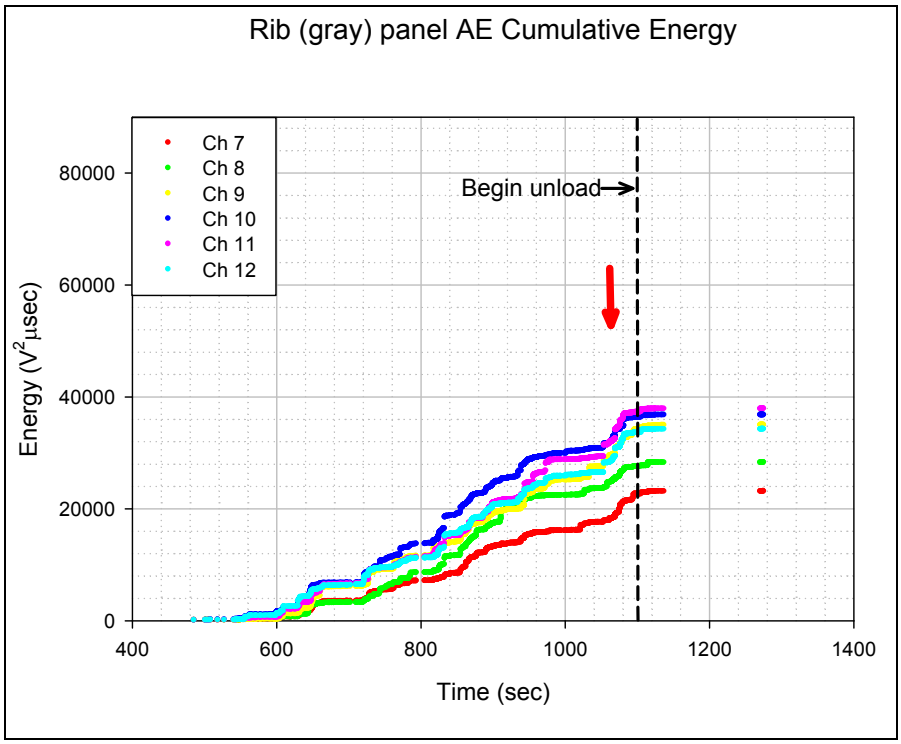

Figure 19. Pressure 2P Test: Gray rib panel AE energy

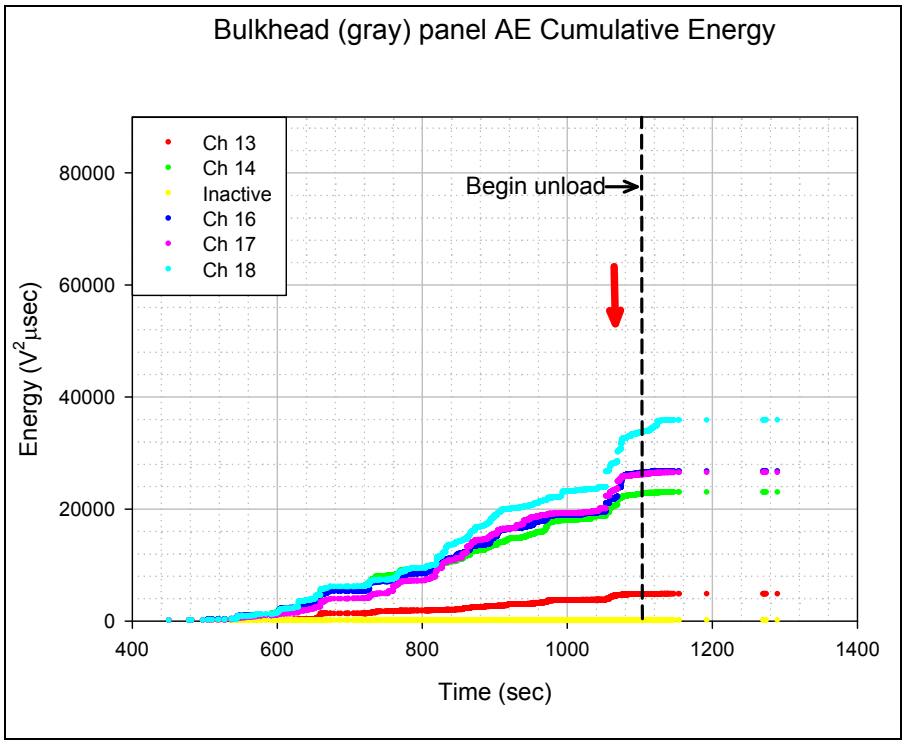

Figure 20. Pressure 2P Test: Gray bulkhead panel AE energy

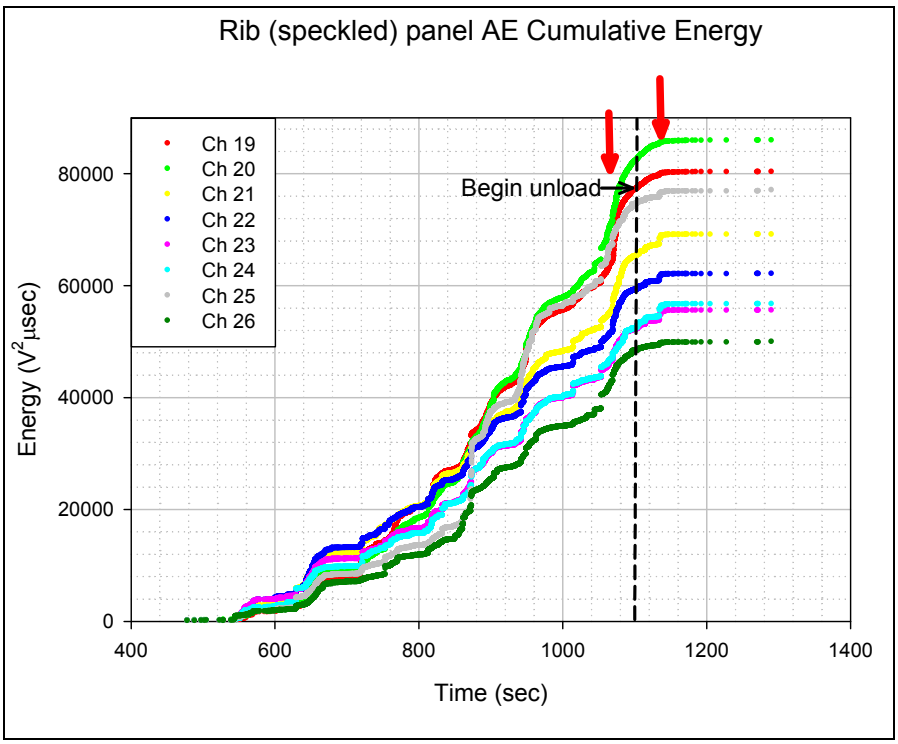

Figure 21. Pressure 2P Test: Speckled rib panel AE energy

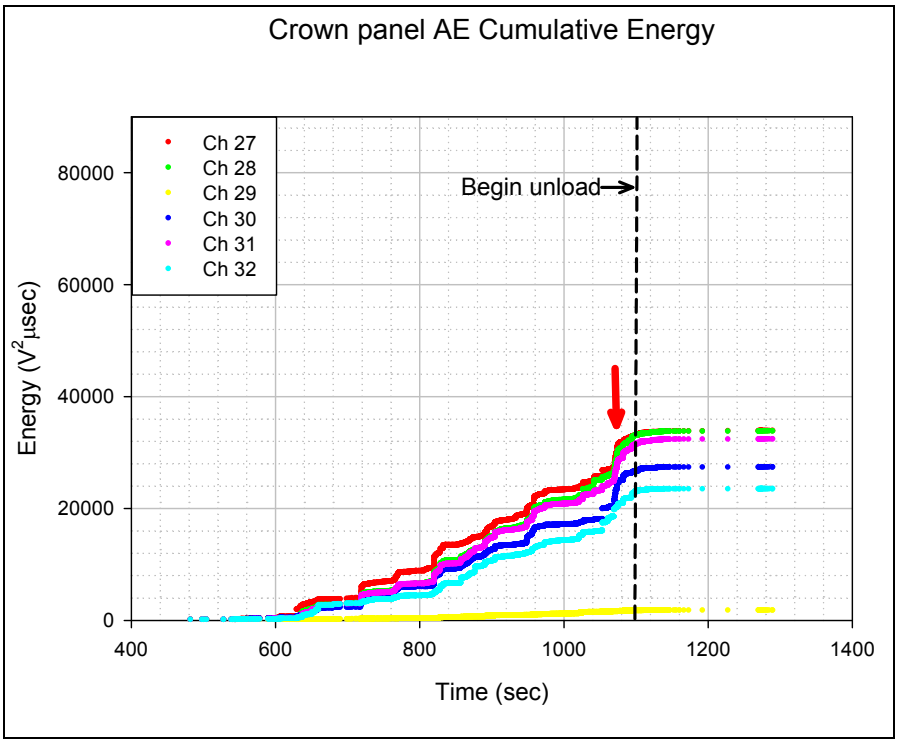

Figure 22. Pressure 2P Test: Crown panel AE energy

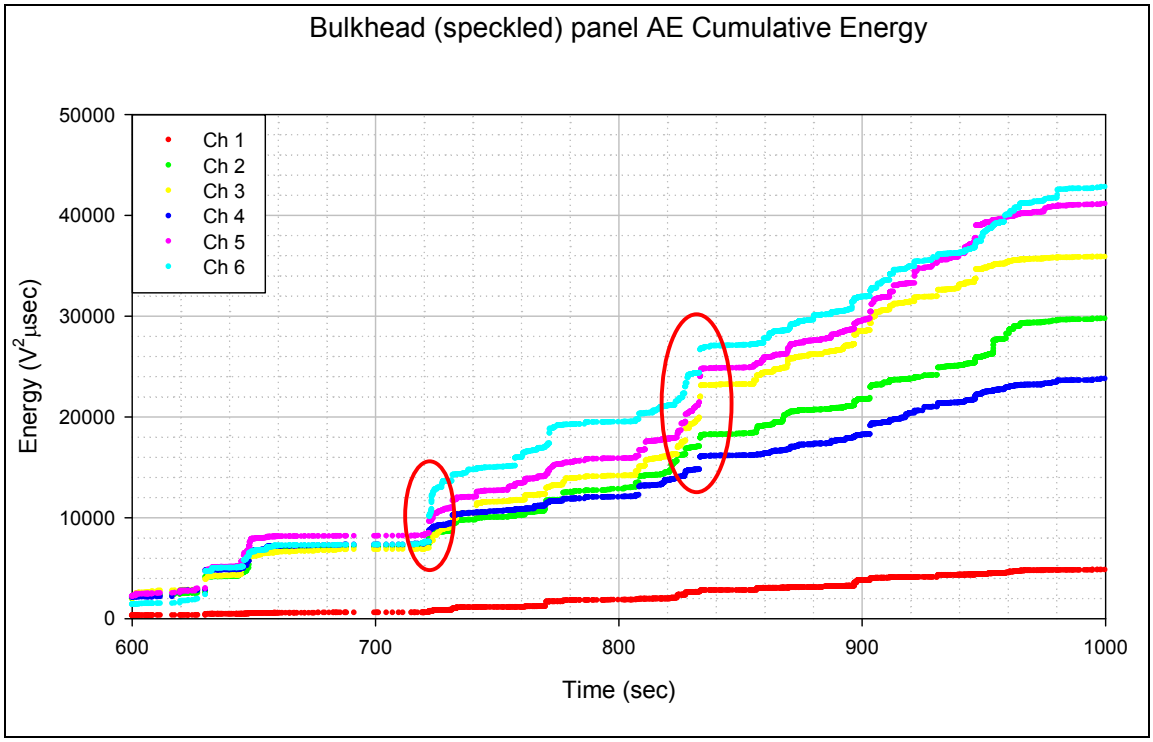

Figure 23. Pressure 2P Test: Close-up of speckled bulkhead panel AE energy near window of strain gage activity

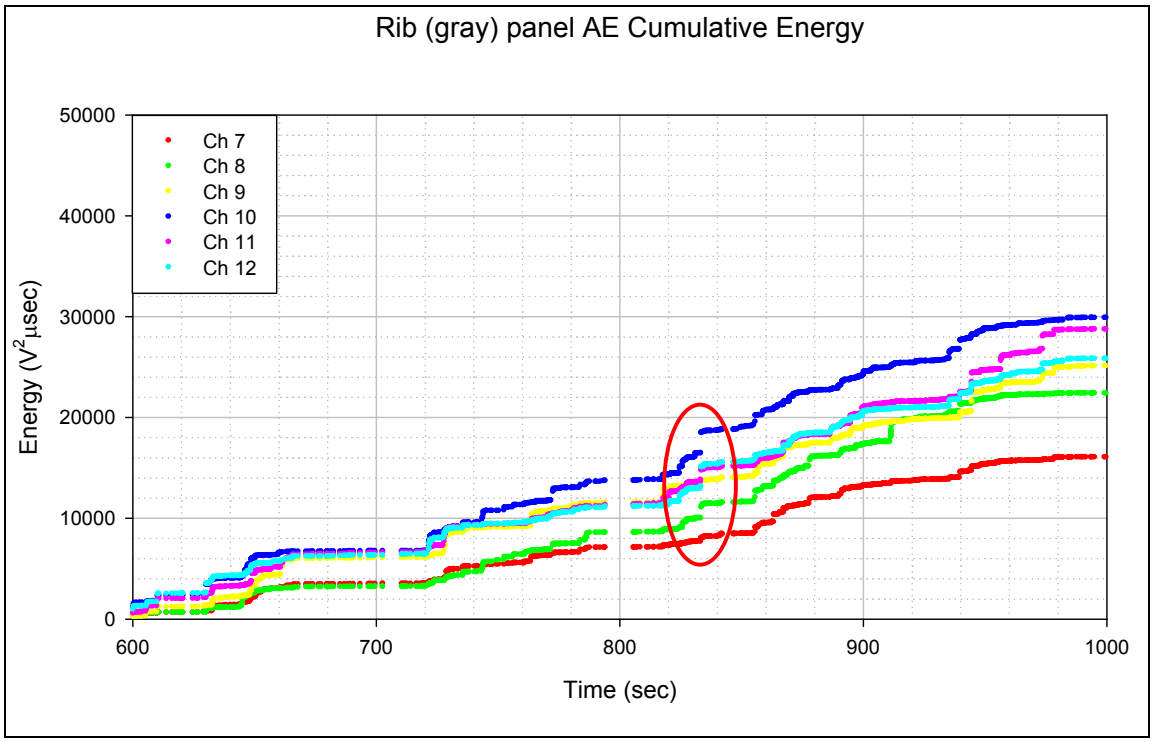

Figure 24. Pressure 2P Test: Close-up of gray rib panel AE energy near window of strain gage activity

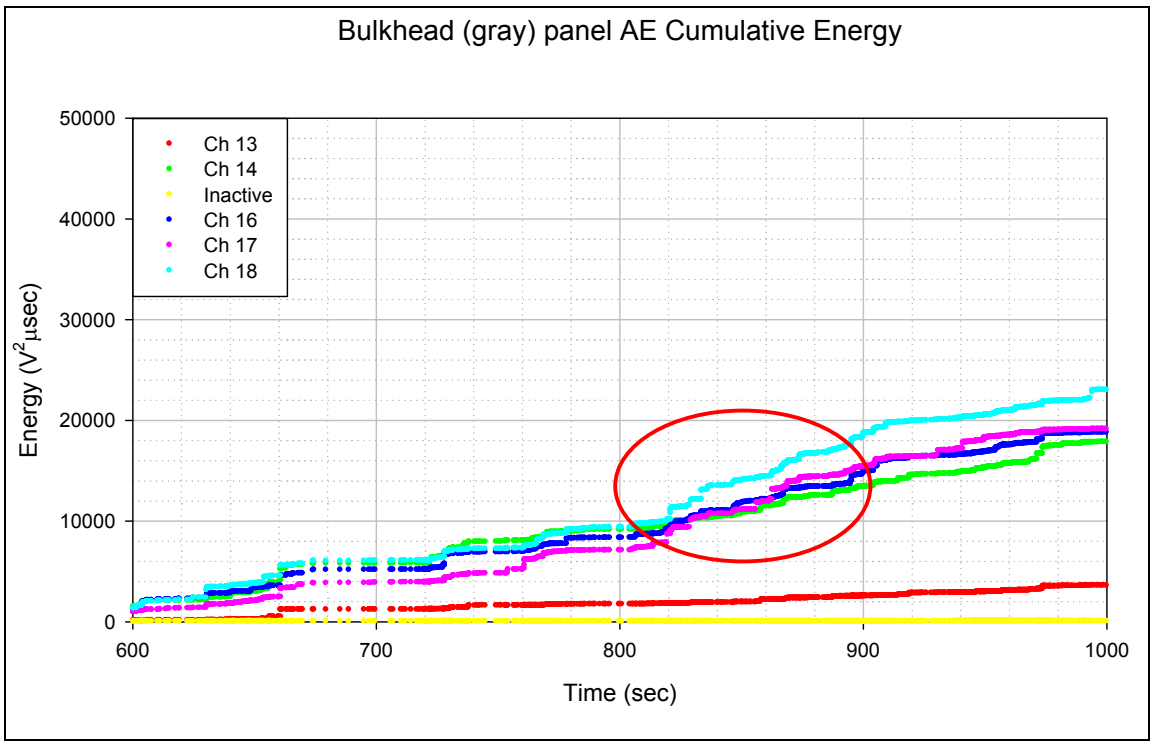

Figure 25. Pressure 2P Test: Close-up of gray bulkhead panel AE energy near window of strain gage activity

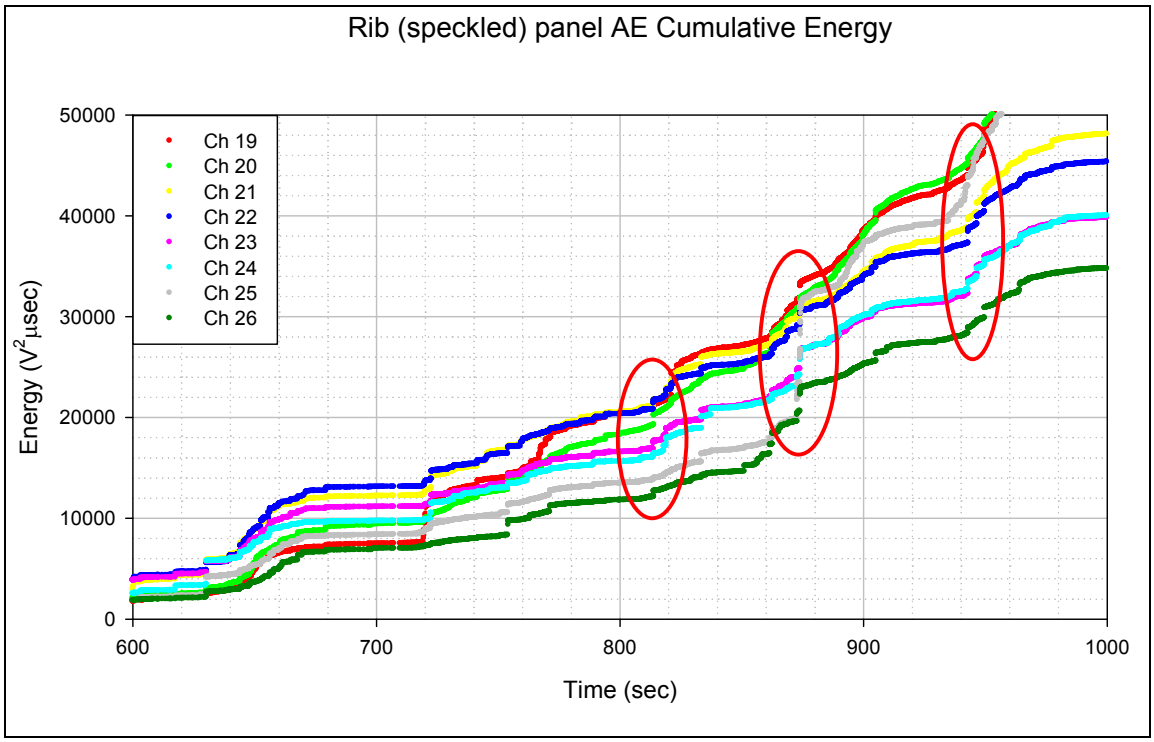

Figure 26. Pressure 2P Test: Close-up of speckled rib panel AE energy near window of strain gage activity

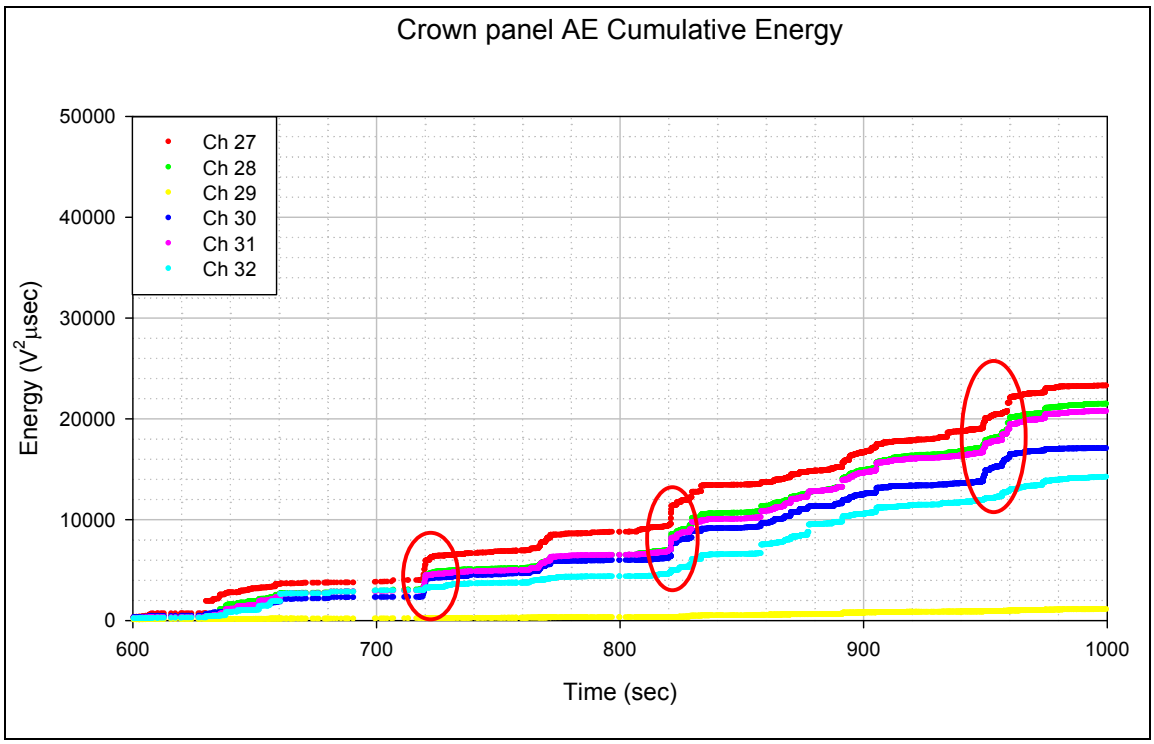

Figure 27. Pressure 2P Test: Close-up of crown panel AE energy near window of strain gage activity

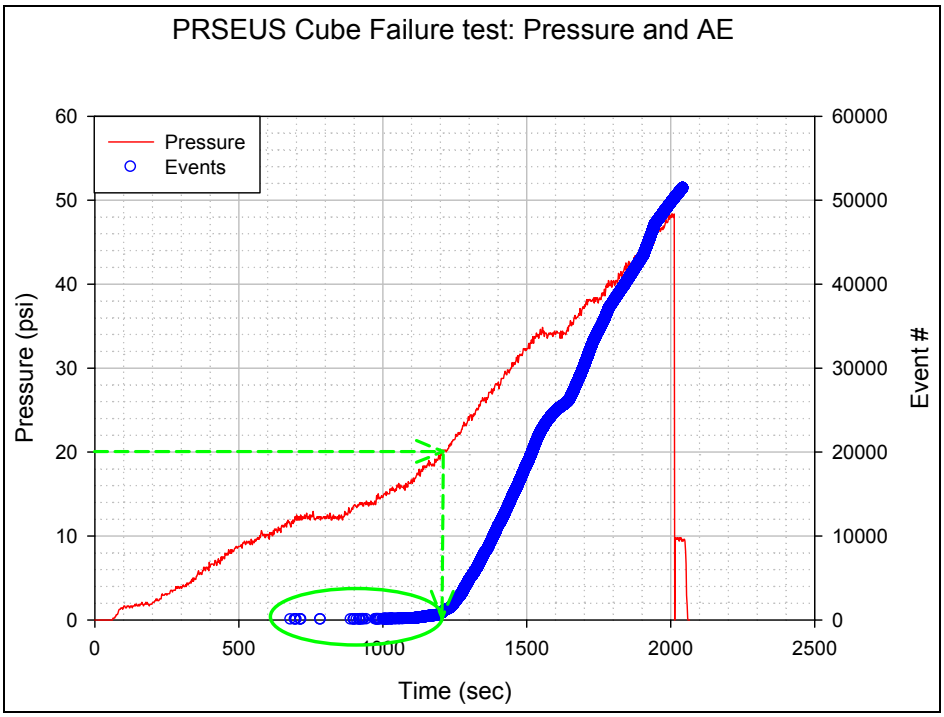

Figure 28. Failure Pressure Test Load profile and AE events

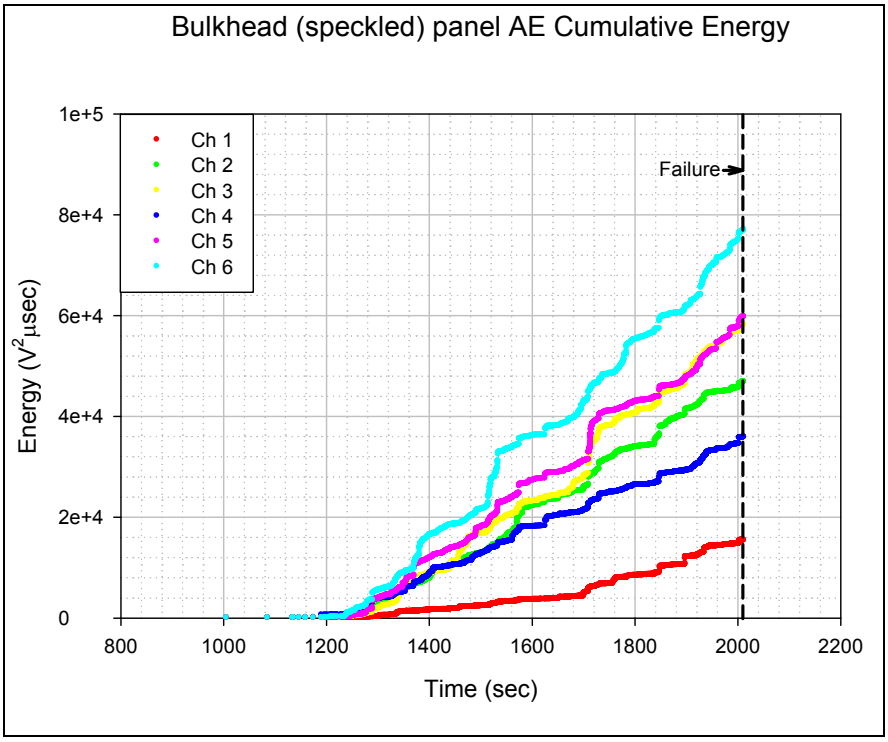

Figure 29. Failure Pressure Test: Speckled bulkhead panel AE energy

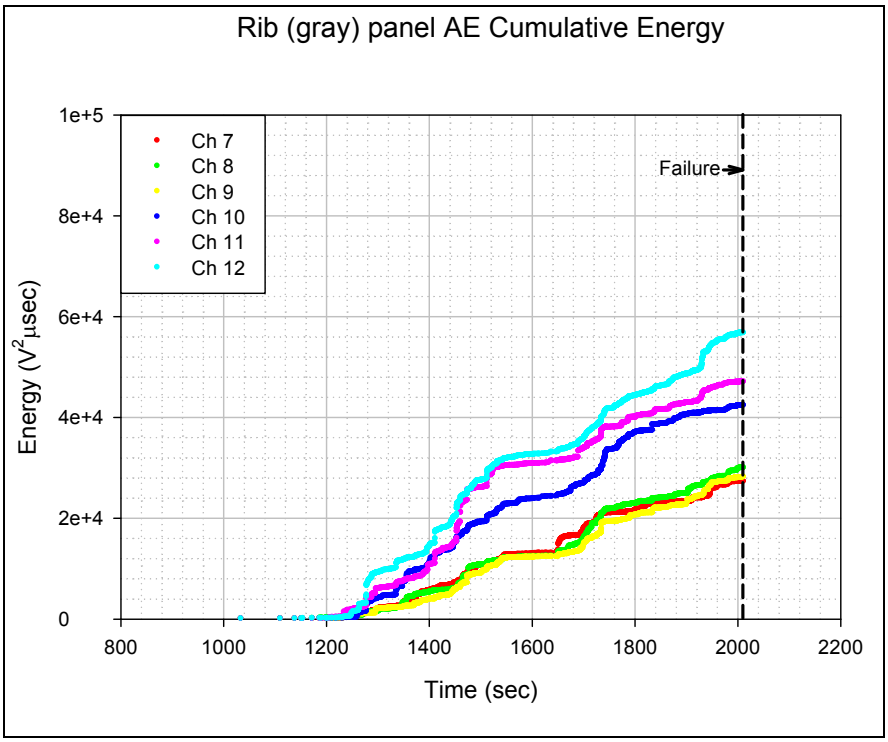

Figure 30. Failure Pressure Test: gray rib panel AE energy

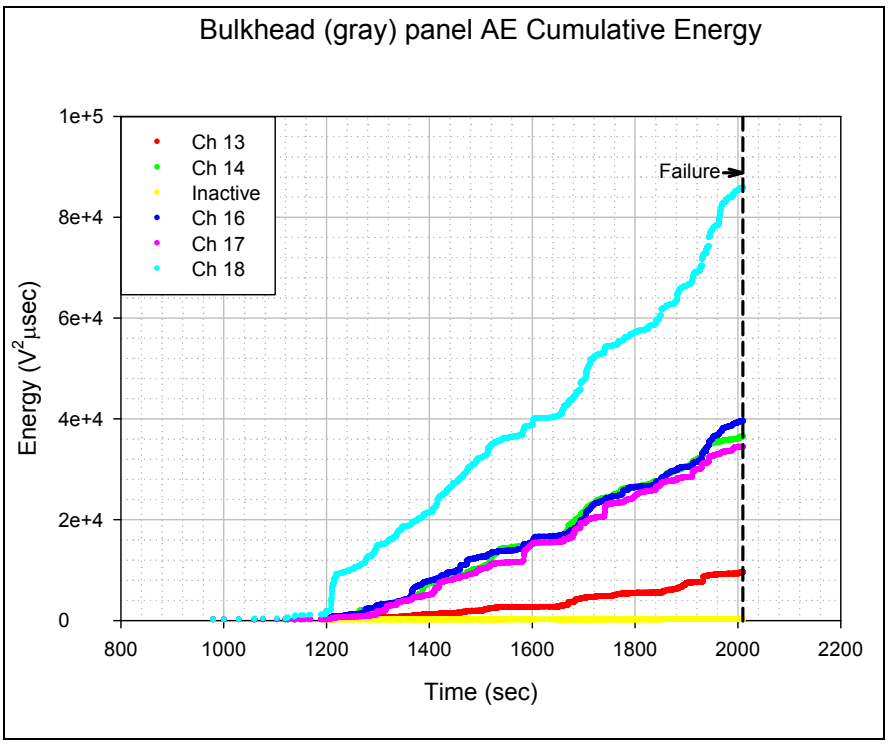

Figure 31. Failure Pressure Test: Gray bulkhead panel AE energy

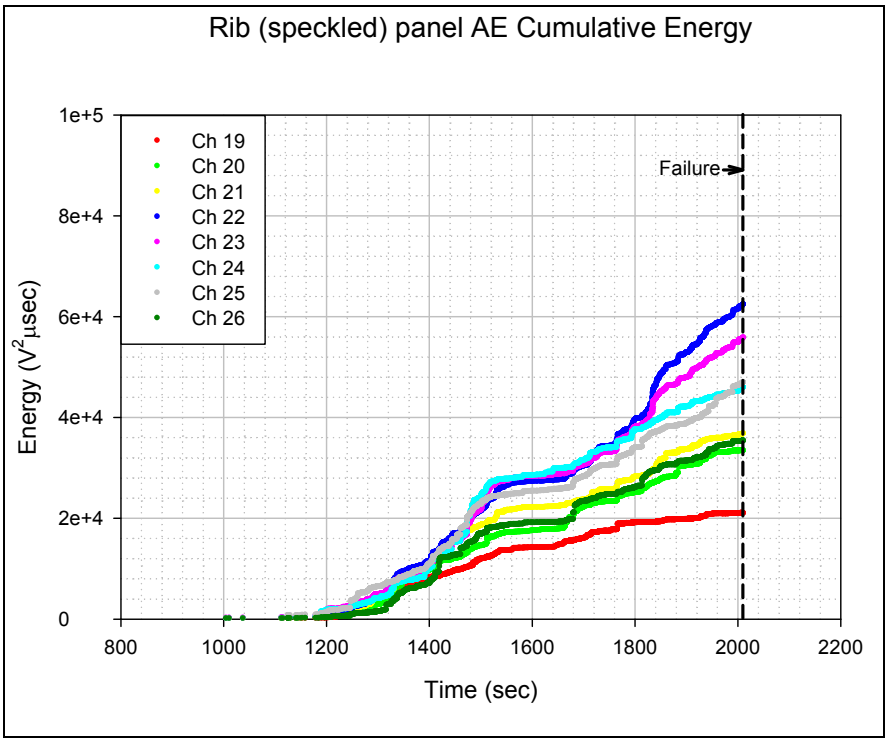

Figure 32. Failure Pressure Test: Speckled rib panel AE energy

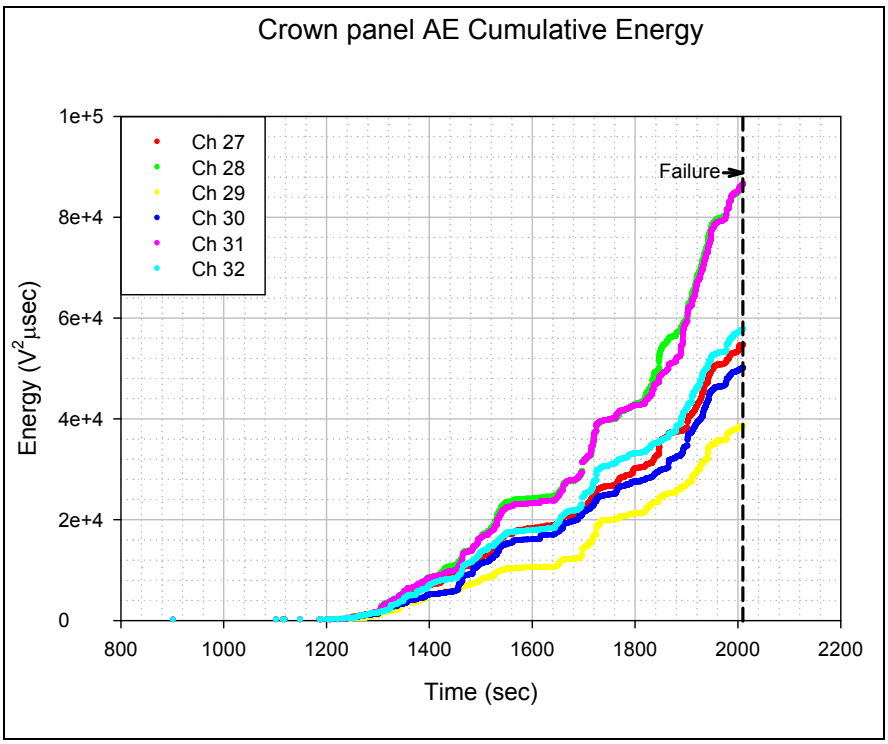

Figure 33. Failure Pressure Test: Crown panel AE energy

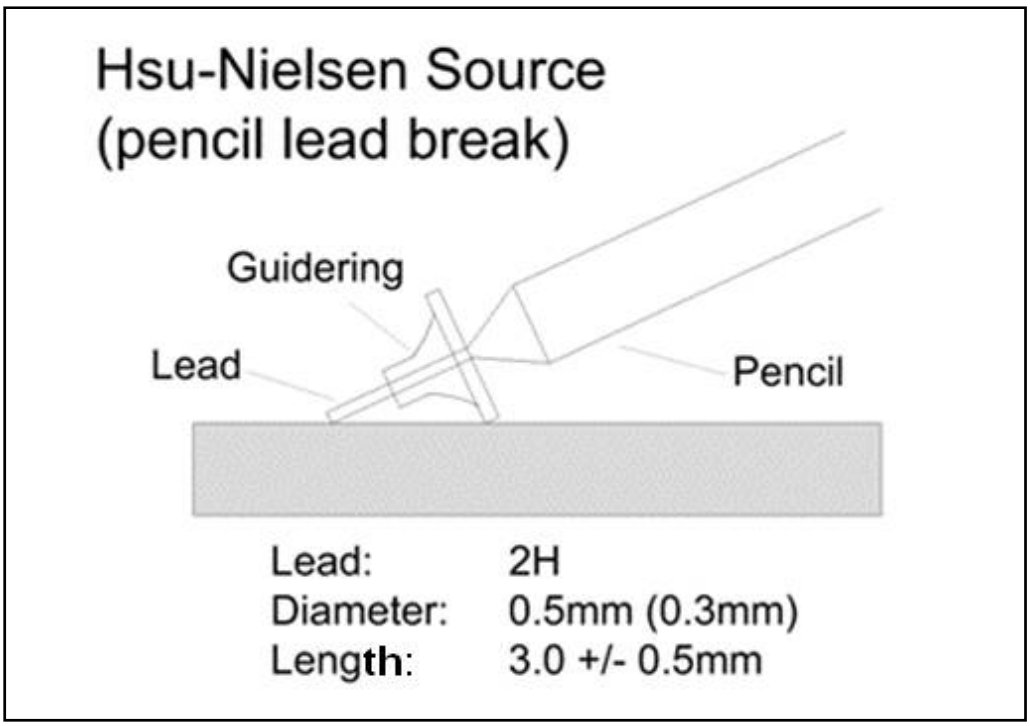

Figure 34. Pencil lead break configuration [9]

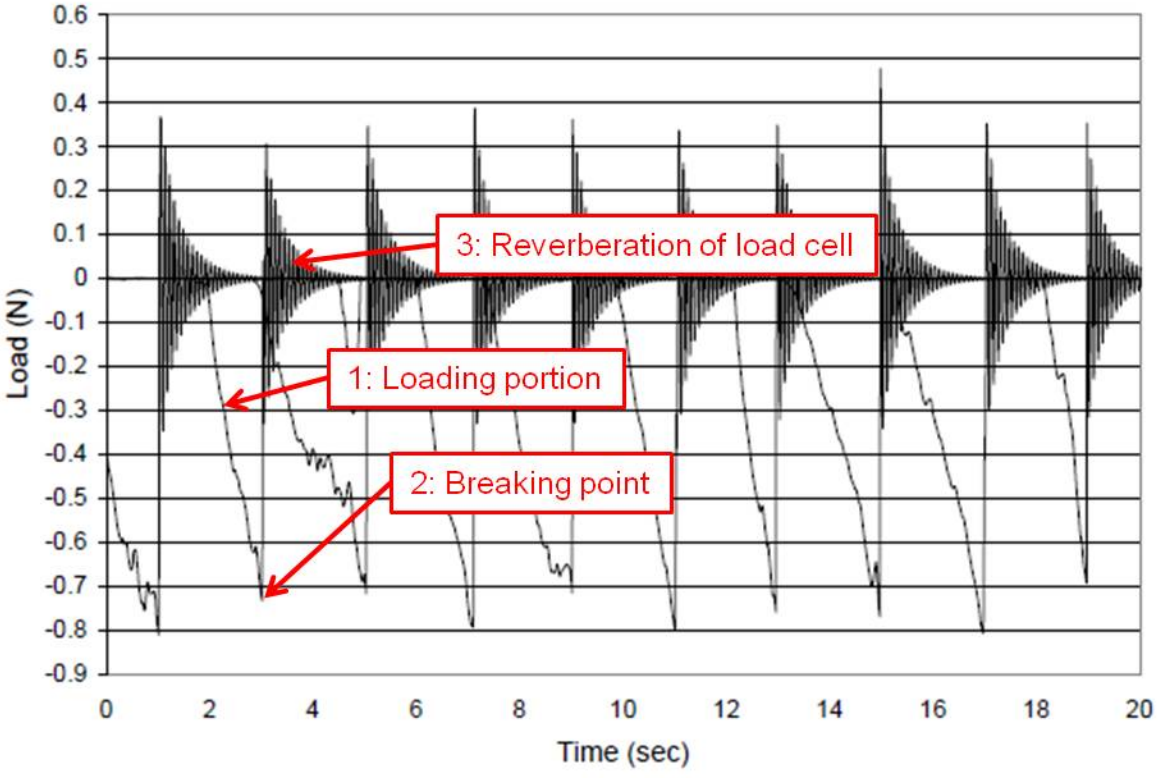

Figure 35. Pencil lead break repeatability [7]

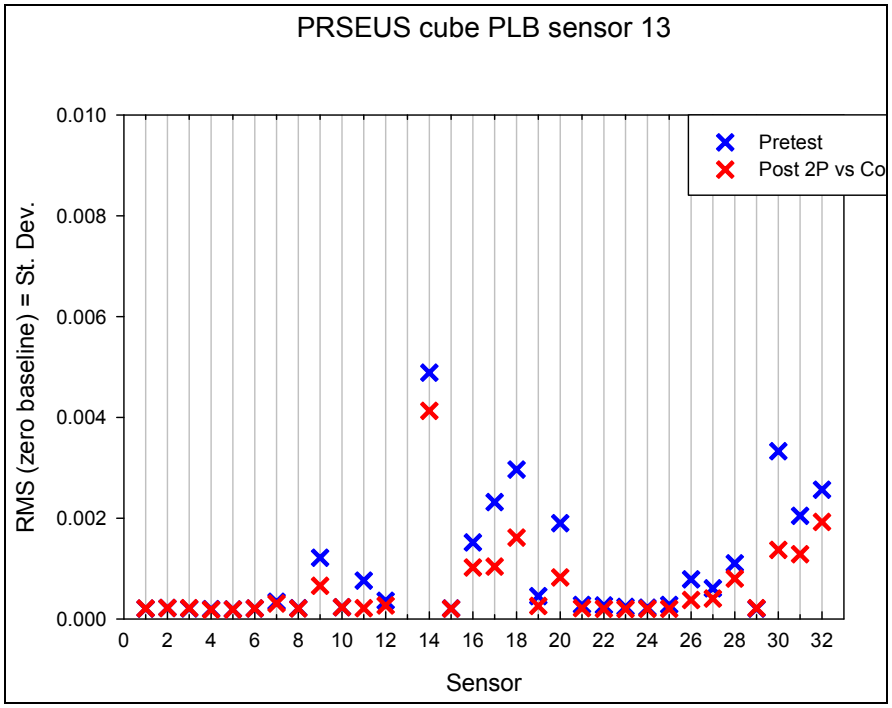

Figure 36. Change in response with damage accumulation of PLB at sensor 13

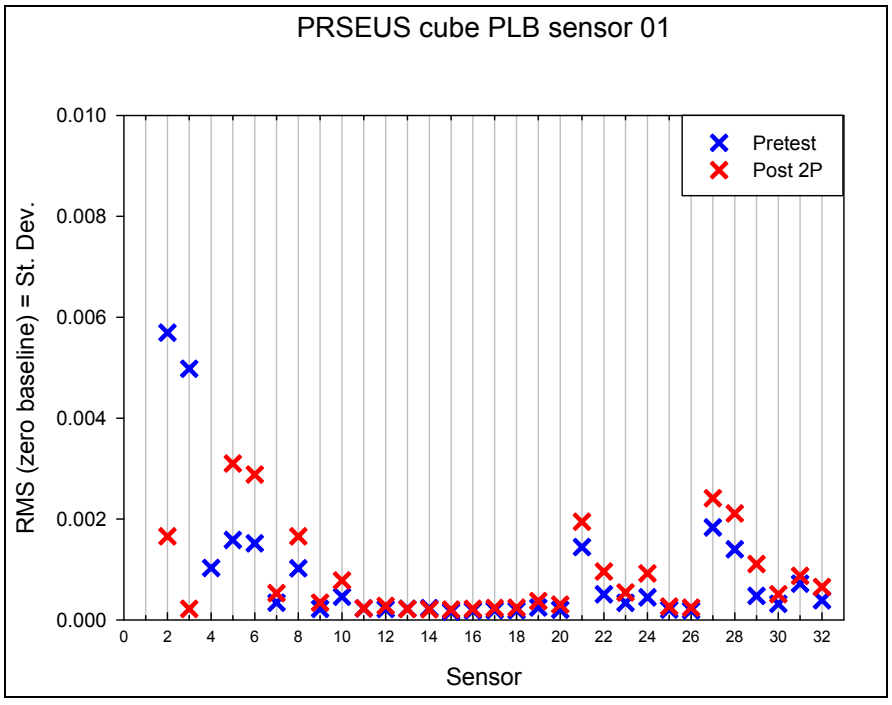

Figure 37. Change in response with damage accumulation of PLB at sensor 1

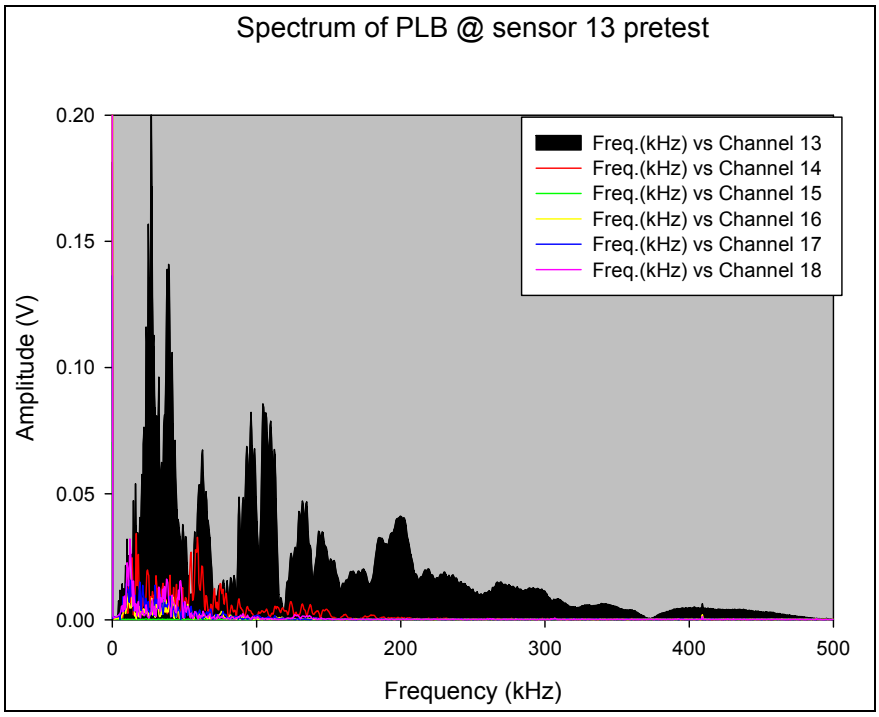

Figure 38. Spectra of initial response of PLB at sensor 13

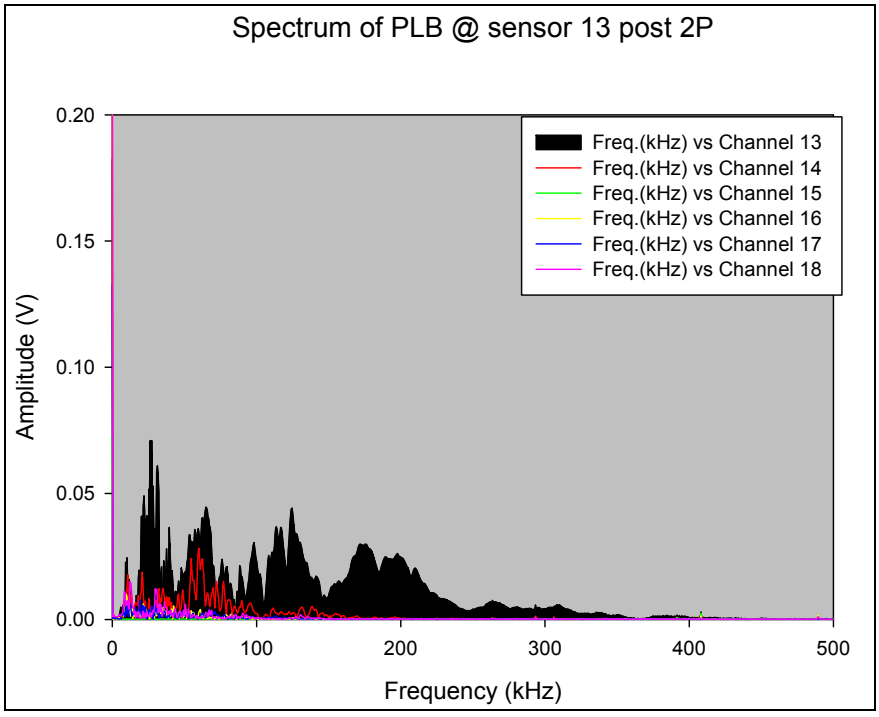

Figure 39. Spectra of response with damage accumulation of PLB at sensor 13

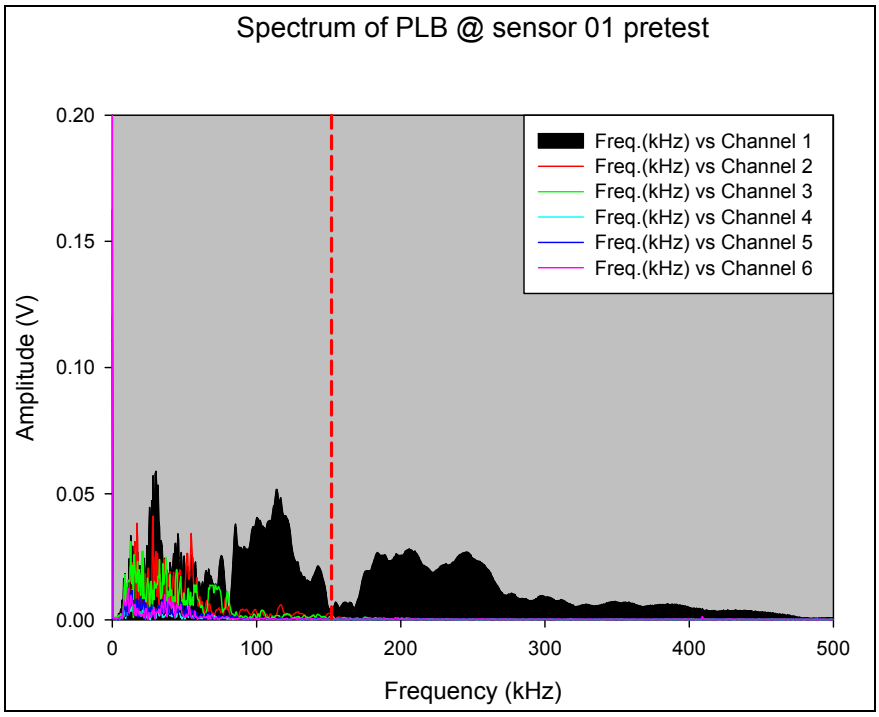

Figure 40. Spectra of initial response of PLB at sensor 1

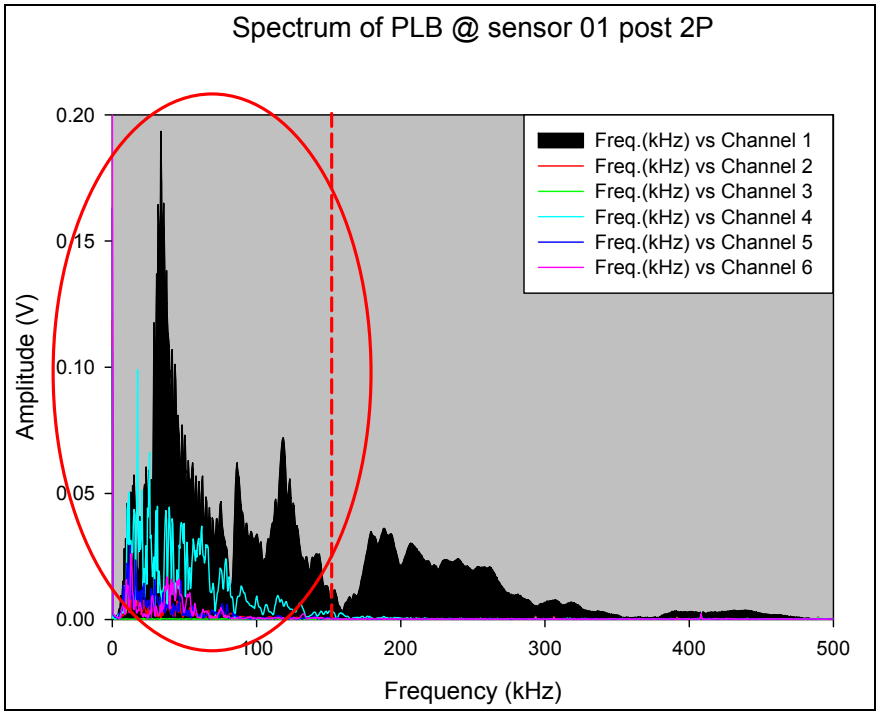

Figure 41. Spectra of response with damage accumulation of PLB at sensor 1

REPORT DOCUMENTATION PAGE

Form Approved
OMB No. 0704-0188

1. REPORT DATE *(DD-MM-YYYY)*	2. REPORT TYPE	3. DATES COVERED *(From - To)*
01- 05 - 2013	Technical Memorandum	

4. TITLE AND SUBTITLE

Evaluation of Acoustic Emission SHM of PRSEUS Composite Pressure Cube Tests

5a. CONTRACT NUMBER

5b. GRANT NUMBER

5c. PROGRAM ELEMENT NUMBER

6. AUTHOR(S)

Horne, Michael R.; Madaras, Eric I.

5d. PROJECT NUMBER

5e. TASK NUMBER

5f. WORK UNIT NUMBER

699959.02.08.07.03

7. PERFORMING ORGANIZATION NAME(S) AND ADDRESS(ES)

NASA Langley Research Center
Hampton, VA 23681-2199

8. PERFORMING ORGANIZATION REPORT NUMBER

L-20227

9. SPONSORING/MONITORING AGENCY NAME(S) AND ADDRESS(ES)

National Aeronautics and Space Administration
Washington, DC 20546-0001

10. SPONSOR/MONITOR'S ACRONYM(S)

NASA

11. SPONSOR/MONITOR'S REPORT NUMBER(S)

NASA/TM-2013-217993

12. DISTRIBUTION/AVAILABILITY STATEMENT

Unclassified - Unlimited
Subject Category 38
Availability: NASA CASI (443) 757-5802

13. SUPPLEMENTARY NOTES

14. ABSTRACT

A series of tests of the Pultruded Rod Stitched Efficient Unitized Structure (PRSEUS) pressure cube were conducted during third quarter 2011 at NASA Langley Research Center in the Combined Loads Test facility (COLTS). This is a report of the analysis of the Acoustic Emission (AE) data collected during those tests. The AE signals of the later tests are consistent with the final failure progression through two of the pressure cube panels. Calibration tests and "damage precursor" AE indications, from preliminary checkout pressurizations, indicated areas of concern that eventually failed. Hence those tests have potential for vehicle health monitoring.

15. SUBJECT TERMS

Acoustic emission; Blended wing body; Composite pressure cube; PRSEUS; Signal energy rate

16. SECURITY CLASSIFICATION OF:			17. LIMITATION OF ABSTRACT	18. NUMBER OF PAGES	19a. NAME OF RESPONSIBLE PERSON
a. REPORT	b. ABSTRACT	c. THIS PAGE			STI Help Desk (email: help@sti.nasa.gov)
					19b. TELEPHONE NUMBER *(Include area code)*
U	U	U	UU	43	(443) 757-5802